Grid Impact of Unbalanced Phase Integration of PV Generation, Electrified Mobility, and Heating in LV Distribution Grids

Wesseling, Yme; Damianakis, Nikolaos; Mouli, Gautham Ram Chandra; Bauer, Pavol

DOI
10.1109/ACCESS.2025.3555169

Publication date
2025

Document Version
Final published version

Published in
IEEE Access

Received 26 February 2025, accepted 23 March 2025, date of publication 26 March 2025, date of current version 7 April 2025.

Digital Object Identifier 10.1109/ACCESS.2025.3555169

RESEARCH ARTICLE

Grid Impact of Unbalanced Phase Integration of PV Generation, Electrified Mobility, and Heating in LV Distribution Grids

YME WESSELING[1], (Member, IEEE), NIKOLAOS DAMIANAKIS[2], (Member, IEEE), GAUTHAM RAM CHANDRA MOULI[2], (Member, IEEE), AND PAVOL BAUER[2], (Senior Member, IEEE)

[1]Movares Nederland B.V., 3511 SX Utrecht, The Netherlands
[2]Department of Electrical Sustainable Energy, Delft University of Technology, 2628 CD Delft, The Netherlands

Corresponding author: Nikolaos Damianakis (N.Damianakis@tudelft.nl)

This work was supported by the Dutch Research Council (NWO) as part of the ongoing Research Project "New Energy and mobility Outlook for the Netherlands (NEON)" of the Research Program Crossover under project number 17628.

ABSTRACT Low-carbon technologies (LCTs) such as Electric vehicles (EVs), heat pumps (HPs), and PV systems increase phase unbalance due to uneven phase distribution. Phase unbalance can lead to overheating, suboptimal capacity utilization, and power losses. This work analyzes the unbalance impact inflicted by the grid integration of PVs, HPs, and EVs under different combinations and penetration levels. The main novelty of this study is the use of different types of real-world distribution grids (rural, suburban, and urban) for the LCT unbalance impact comparison, while simultaneously considering the influence of several unbalance factors; LCT phase connections and grid distributions, the seasonal effect, and the power and consumption levels, the latter of which have been evaluated as mitigation strategies. The results showed that the combined integration of PVs, EVs, and HPs can cause high voltage unbalance, especially in grids with high existing loading. The seasonal effect was the most impactful unbalance factor, intensifying unbalance by the integration of PVs-HPs and PVs-EVs combinations during Winter and Summer, respectively. Furthermore, reductions in the power and consumption levels of the LCTs decreased the unbalance total violation duration in a range between 11% and 25% for all distribution grids. Reducing the LCT consumption levels also decreased the unbalance magnitude, which reached up to 15% for the urban grid under 100% HP and PV penetration. Finally, it was found that consumption duration enhances unbalance, such as the peak power levels, because it increases the simultaneity of technologies operating in different phases.

INDEX TERMS Distribution grids, electric vehicles, grid impact, heat pumps, PVs, voltage unbalance.

NOMENCLATURE

Δt	Timestep.
$\dot{m}_{wat}$	Flow Water Rate of the Heat Pump.
$\dot{Q}_{cond}$	Conduction Losses.
$\dot{Q}_{hp}$	Heat Pump Output.
$\dot{Q}_{ir}$	Heat by Irradiation.
$\dot{Q}_{los}$	Heating Losses.
$\dot{Q}_{vent}$	Ventilation Losses.
$\eta^{25^oC,G_{inc}}$	PV Efficiency under Module Temperature 25^oC and Irradiation G^{inc}.
η^{inv}	PV Inverter Efficiency.
η^{PV}	Real PV Efficiency.
$\eta^{T_M,G_{stc}}$	PV Efficiency under Module Temperature T_M and Irradiation G^{stc}.
η_{stc}	PV Module efficiency under STC.
ρ_{air}	Air Density.
θ_M	PV Module's Tilt Angle.
θ_s	Solar Elevation Angle.
A_M	Module Area.
af	Absorptivity Factor.

The associate editor coordinating the review of this manuscript and approving it for publication was Giambattista Gruosso.

Az_M	PV Module's Azimuth.
B_{ev}	EV's Battery Capacity.
c_η	Temperature Coefficient of PV Efficiency.
C_{air}	Air specific Capacity.
C_b	Building Thermal Capacity.
$c_{P_{MPP}}$	Temperature Coefficient of MPP PV Power.
C_{wat}	Water specific Capacity.
E_i	Yearly Energy Consumption of Building *i*.
E_r	EV's Requested Energy.
FF	Fill Factor of PV Module.
G^{stc}	Irradiance under STC.
G_{inc}	Incident Irradiance.
G_{noct}	Irradiance under NOCT.
$I_{SC}^{25^oC,G^{inc}}$	PV Module S-C Current under Module Temperature 25^oC and Irradiation G^{inc}.
I_r	EV's Rated Current.
I_{ch}	EV's Charging Current.
I_{cv}	EV's CV Charging Current.
$P_{MPP}^{25^oC,G^{inc}}$	MPP PV Power under Module Temperature 25^oC and Irradiation G^{inc}.
P_{MPP}^{stc}	MPP PV Power under STC.
$P_{MPP}^{T_M,G^{stc}}$	MPP PV Power under Module Temperature T_M and Irradiation under STC.
P_d	Base Load Distribution Profile Power.
P_l	Base Load Consumption Power.
P_{hp}	HP Consumption Power.
P_{pv}	PV Generation Power.
s_w	Wind speed.
T_a	Ambient Temperature.
T_M	PV Module's Temperature.
T_p	EV's Parking Time.
T_b	Building Temperature.
T_{noct}	Temperature under NOCT.
T_{ret}	HP Return Water Temperature.
T_{sup}	HP Supply Water Temperature.
$V_{OC}^{25^oC,G^{inc}}$	PV Module O-C Voltage under Module Temperature 25^oC and Irradiation G^{inc}.
V_n/V_p	Negative/Positive Sequence Voltage.
V_{ab}, V_{bc}, V_{ca}	Three Phase-to-phase Voltages.
V_b	Building Volume.

ABBREVIATIONS

AOI	Angle of Incidence.
BESS	Battery Energy Storage System.
CC	Constant Current (Charging Region).
COP	Coefficient of Performance.
CV	Constant Voltage (Charging Region).
DG	Distribution Grid.
DHW	Domestic Hot Water.
DSM	Demand Side Management.
DSO	Distribution System Operator.
ESS	Energy Storage System.
EV	Electric Vehicle.
HP	Heat Pump.
LCT	Low-Carbon Technology.
LV	Low Voltage.
MCS	Monte-Carlo Simulation.
MPP	Maximum Power Point.
MV	Medium Voltage.
NOCT	Normal Operation Conditions Test.
O-C	Open Circuit.
PV	Photovoltaics.
S-C	Short-Circuit.
SOC	State of Charge.
STC	Standard Test Conditions.
T/F	Transformer.
VUF	Voltage Unbalance Factor.

I. INTRODUCTION

The European Green Deal established the aim of net zero greenhouse gas emissions in the EU by 2050 [1]. To reach this goal, low carbon technologies (LCTs) such as heat pumps (HPs), electric vehicles (EVs), and PV rooftop systems will be abruptly increased in the residential and commercial sectors [2], [3], [4], due to the transition to sustainable energy and new emission regulation policies [5].

However, the integration of LCTs will increase the strain on the distribution grid (DG), which is already near the energy transport capacity limits in many countries such as the Netherlands [6]. Apart from the impact on grid capacity, adopting LCTs can increase phase unbalance since many of these components will be connected to a single phase of the three-phase distribution network. This is because most LCTs, such as residential PV rooftops and HPs, are low power level components and do not exceed 3 kW-rated power [7].

Phase unbalance occurs when there is a deviation in voltage, current, or phase angle between the three phases. Several reasons can cause phase unbalance. Firstly, as already stated, the uneven distribution of single-phase customers with uneven loading over the three phases, as well as their stochastic load behavior, e.g. concerning HP operation or EV charging [8], can have a serious impact on phase unbalance. For example, while Dutch public and commercial buildings built since 2010 have a 3-phase connection, most households constructed before 2010 are single-phase connected [9]. Secondly, structural asymmetries in distribution grids can jeopardize the grid balance due to uneven line self and mutual impedance [10]. Finally, unbalanced faults such as line-to-line short circuits (SC), line or double line-to-ground SC & broken lines can seriously harm system balance [11].

Phase unbalance is undesirable since it inflicts various serious consequences for the distribution grid. The unequally distributed voltages or currents over the phases can lead to a higher peak power than necessary. Since the required capacity must be increased to accommodate the higher peak values, the reinforced grid capacity is not fully and, hence, sub-optimally utilized [10]. Moreover, the cost of this reinforcement can be considerable, as quantified in [12]. Finally, another consequence of unbalance is increased thermal and power

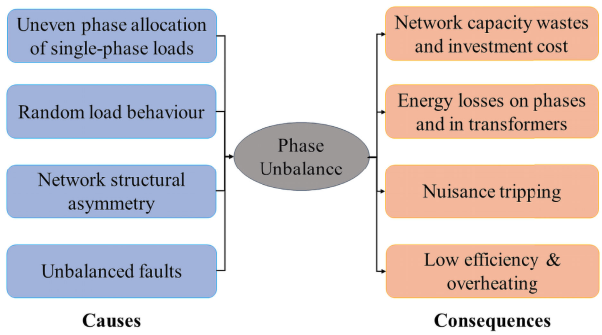

FIGURE 1. Causes and consequences of phase unbalance [10].

losses and overheating in the power cables. One main reason is the flowing current in the neutral wire under phase unbalance conditions [10]. The causes and consequences of unbalance are summarized in FIGURE 1 [10]. This work evaluates the impact of the integration of PVs, HPs & EVs on phase unbalance in different types of Dutch low-voltage (LV) distribution grids (rural, suburban, and urban) under different combinations and penetration levels. Moreover, the influence of four main unbalance factors has been analyzed: the LCT phase connections and grid distributions, the seasonal effect, and finally, the LCT power and consumption levels which have also been investigated as unbalance mitigation strategies. The mean and maximum voltage unbalance factor (VUF) has been utilized for the phase unbalance analysis.

II. LITERATURE OVERVIEW AND CONTRIBUTIONS

A. IMPACT OF INDIVIDUAL LCT INTEGRATION ON PHASE UNBALANCE

Several existing works studied the impact of PV integration on phase unbalance. The impact of single-phase rooftop PV installations on LV distribution networks was investigated using probabilistic simulations in [13]. The study randomized the location and phase connection of the PV installations and the rated power and penetration levels. It was found that while increased penetration of small single-phase PV systems (5 kW) can stabilize voltage unbalance in the network, larger single-phase PV systems (15 kW) can increase voltage unbalance in the distribution grids. Similar results about phase unbalance increase or reduction depending on the power output of the PV systems were observed in the studied worst-case scenarios in [14]. However, the analysis was conducted in a developed representative LV network feeder and not in real grid case studies. Additionally, a large PV field's impact on a Torino building was studied in [15] using various unbalance metrics, highlighting the importance of partial shading on current unbalance. Finally, various unbalance metrics were used in [16] for voltage unbalance regulation in different LV distribution grids.

Concerning unbalanced EV integration, uncontrolled and tariff-based control case studies were investigated in [17]. While voltage unbalance was introduced from 50% penetration in the uncontrolled study, the tariff-based control managed to suppress it. Additionally, the impact of a workplace parking lot with 54 EV chargers in Tunisia was analyzed in [18]. While voltage unbalance remained below the standard limit at all times, EV chargers introduced significant current unbalance. Furthermore, a mixed-integrated linear programming approach was proposed in [19] for two uncontrolled EV charging methods, which reduced the power losses for up to 14.8%. Moreover, it was shown that a considerable amount of power losses can be concealed if the neutral conductor is not considered in unbalanced simulations. On the contrary, the authors in [20] utilized EV fleets with vehicle-to-grid capabilities to improve grid stability and power quality minimizing active power losses and voltage deviations. Finally, the importance of using unbalanced power flows for grid impact assessment has been proven in the probability study [21], which investigated different types of HP integration in LV distribution grids.

B. IMPACT OF COMBINED LCT INTEGRATION ON PHASE UNBALANCE

Regarding the combined impact of unbalanced LCT integration, unbalance induced by combined PVs-EVs integration has been investigated the most. EV charging was found more hazardous than PV generation for voltage unbalance of the IEEE residential feeder of [22] and the Irish LV grids of [23] while the use of demand side management (DSM) and battery energy storage systems (BESS) was proposed, respectively. Moreover, the impact of EV charging location and mode on voltage unbalance variations with simultaneous PV integration has been proven in the probabilistic analysis of [24]. Additionally, the impact of increasing EVs-PVs penetration levels has been analyzed in [25] and [26], where January and August were found to be the most hazardous months and rural networks were found to be the most vulnerable, respectively. Furthermore, the related unbalance impact was translated to total imbalance-induced cost concerning energy losses and capacity wastes in [27] while the impact of unbalance on the residential smart grid performance was evaluated in [28]. On the contrary, the studies of [29] and [30] investigated the combination of EVs and HPs under various penetration levels on voltage unbalance. In [29], it was shown that the integration of EV chargers has a more significant effect on the voltage unbalance, while in [30], the importance of newer buildings with higher energy labels was proven. Finally, [31] studied the HPs-PVs combined integration for unbalance mitigation in rural and urban grids.

Few works have also focused on the impact of the combined integration of PV, EVs, and HPs on unbalance, such as [32], [33], and [34]. In [32], it was shown that the distribution network could tolerate integrating LCTs separately. However, the integration of EV chargers caused significant voltage unbalance, due to the large variability in demand compared to HPs. Moreover, the significance of the number of customers in the distribution feeders was shown in [33] while the importance of the customers' location in the grid was identified in [34]. However, none of these works investigated the effect of different types of distribution grids in combination with the seasonal effect and different power levels when all PVs, EVs, and HPs are integrated under different penetrations.

C. RESEARCH GAP AND CONTRIBUTIONS

The existing works that have assessed the grid unbalance impact of the combined LCT integration are summarized in TABLE 1. It can be seen that only a few phase unbalance assessment works have incorporated all PVs, EVs, and HPs in their study, while season comparison has only been investigated in [25]. While works such as [31] and [33] have conducted analysis of several months, the phase unbalance was analyzed for the total duration neglecting the seasonal interrelations of the investigated LCTs and their influence on the phase unbalance in different seasons.

On the one hand, the effect of the random LCT grid distribution on phase unbalance under multiple penetrations has only been studied in [24], [30], [31], and [33]. On the other hand, comparisons of different types of grids (e.g. rural, suburban, urban, etc) have only been conducted in [26], [27], [31], and [34]. From these sets of works, only [33] and [34], respectively, comprise the integration of PVs, EVs, and HPs, while none of the existing works analyze them together utilizing real-world grid case studies.

Furthermore, apart from different LCT phase connections and LCT grid distribution, adjusting the power- and consumption-level of LCTs can have a significant impact on the inflicted phase unbalance and can potentially be used as an unbalance mitigation measure. From the existing works, only [24] and [33] have studied this effect as a mitigation measure, and only for EVs (smart charging use in [24]).

Finally, grid impact assessment studies can follow mainly top-down and bottom-up approaches. While top-down approaches use generalized data scaled down to the level of the investigation, a bottom-up approach generates the needed LCT profile data by utilizing detailed LCT models to incorporate the physical operation of the components and increase scalability, modifiability and consider the effects of simultaneous LCT operation [35]. Overall, this work's contributions are summarized as follows:

1) A bottom-up study that analyzes and compares the phase unbalance inflicted by EVs and HPs in PV-integrated grids under multiple penetrations accounting simultaneously for the influence of the season. This kind of study has only been conducted in [25], which, however, comprised only a comparison of PVs and EVs, whereas [33] neglected the comparison of different seasons. On the one hand, different LCT pairs (PVs-EVs, PVs-HPs) inflict different unbalance on distribution grids due to different simultaneity and operation characteristics, such as duration and power levels. On the other hand, different seasons directly affect the different LCT profiles in bottom-up approaches, increasing and decreasing power peaks and consumption levels. The study of this combined effect is still missing from the existing literature.

2) Investigates and compares the phase unbalance inflicted by LCT integration in different types of grids (namely rural, suburban, and urban) utilizing six real-world (Dutch) distribution grids and considering the existing grid loading and the LCT grid distribution effect. Concerning works that comprise PVs, EVs, and HPs, the effect of LCT grid distribution on phase unbalance has only been investigated in [33], while a comparison of different types of grids is still missing from the literature. The study of this combined comparison under the integration of different LCTs in real-world grids can provide significant insights about the most hazardous LCT depending on the type of the investigated grid and its characteristics and the LCT distribution.

3) Evaluates one power-based and one consumption-based mitigation method for EVs and HPs, respectively, analyzing the effect of different LCT power and consumption levels on phase unbalance. The effect of the LCT power and consumption level on phase unbalance has been accounted for only in [24] and [33] (see TABLE 1); however, only concerning the EV mode of operation, e.g. smart-charging. Moreover, the authors in [27] did not consider HPs in their study, while in [33], it was not assessed as a potential phase unbalance mitigation measure.

The rest of this work is categorized as follows. Section III integrates the methodology of this work, thus the modeling of the LCTs and their phase connections. Section IV includes the case studies, LCT grid distribution and simulation setup. Sections V & VI comprise the results and discussion, respectively, where the work's findings are compared with the existing knowledge and recommendations are given for critical unbalance situations. Finally, Section VII comprises the conclusions and future work recommendations.

III. METHODOLOGY

A. VOLTAGE UNBALANCE FACTOR (VUF)

In this work, the VUF was chosen to quantify three-phase unbalance, which is defined as the ratio between the negative sequence voltage component V_n and the positive sequence voltage component V_p, as shown in (1) where V_{ab}, V_{bc}, V_{ca} the three phase-to-phase voltages of the three phases a, b, c and α the phasor rotation operator [36]. This metric has been chosen. firstly, because it considers both the voltage magnitudes and the voltage angles and is defined as the true definition of voltage unbalance [36]. Secondly, it is the most commonly used metric in the literature, and its utilization for the highest accuracy in estimation is endorsed by multiple studies, such as in [30]. Finally, VUF is the used metric for voltage unbalance limits definition for Dutch DSOs [37]. It must be noted that the legal phase unbalance limits considered in this work (e.g. 3% maximum voltage unbalance) apply for the case of the Netherlands, defined in [7] and [37].

$$\%\text{VUF} = \frac{V_n}{V_p} * 100$$

TABLE 1. Characteristics of existing grid unbalance assessment works with combined LCT consideration.

Ref	PV	EV	HP	Multiple Pen/tions	LCT Comp.	Grid Type Comp.	Real Grids	Season Comp.	LCT Grid Dis/tion Effect	LCT Power & Cons/tion Effect	Mitigation
[28]	✓	✓					✓				
[25]	✓	✓		✓	✓		✓	✓			3P-connection & BESS
[22]	✓	✓			✓						DSM
[23]	✓	✓		✓			✓				BESS
[27]	✓	✓		✓	✓	✓	✓				
[26]	✓	✓		✓	✓	✓					
[24]	✓	✓		✓	✓				✓	✓	smart-charging
[29]		✓	✓	✓							TOU & DR
[30]		✓	✓	✓	✓		✓		✓		
[31]	✓		✓	✓	✓	✓	✓		✓		higher TF cap & 3P-connection & larger cables
[32]	✓	✓	✓		✓						
[34]	✓	✓	✓		✓	✓					
[33]	✓	✓	✓	✓	✓		✓		✓	✓(EVs)	
Work	✓	✓	✓	✓	✓	✓	✓	✓	✓	✓	EV avg charging & HP: thermal comfort decrease

$$V_n = \frac{V_{ab} + \alpha^2 \cdot V_{bc} + \alpha \cdot V_{ca}}{3}$$
$$V_p = \frac{V_{ab} + \alpha \cdot V_{bc} + \alpha^2 \cdot V_{ca}}{3} \quad (1)$$

where $\alpha = 120°$

B. MODELING OF LOADS AND LCTs

As discussed, this work has followed a bottom-up approach. Hence, the LCT profiles were generated with the use of LCT models with reasonable accuracy to consider the component-side view and increase scalability and modifiability. Consequently, the profiles were distributed to the LCTs in the grid simulations according to each case study and penetration level. It must be highlighted that attention has been given to the coupling of the LCT models, and the same data input has been used to create the different LCT profiles, such as weather data for PVs and HPs (e.g. irradiation, ambient temperature, etc.) in order to increase the consistency of the work.

1) BASE LOAD

The base load consumption $P_l^i(t)$ of each grid building i is calculated considering the load yearly consumption E^i and per-minute load residential or commercial distribution profiles $P_d(t)$ from the "Platform Verbruiksprofielen" database [38], as dictated in (2).

$$P_l^i(t) = E^i P_d(t) \quad (2)$$

2) PV SYSTEMS

The PV generation profiles were developed based on [39] and [40]. Each PV rooftop system was rated at 3 kW generation power. The total module incident irradiance G_{AOI} at a certain angle of incidence (AOI) was calculated using the "Isotropic Sky Model" with weather data such as direct normal, diffuse horizontal & global horizontal irradiances, air temperature, and wind speed obtained by the Meteonorm database [41]. The most important equations of the utilized model are summarized below.

$$cos(AOI(t)) = cos(\theta_M)sin(\theta_s(t)) + sin(\theta_M)cos(\theta_s(t))cos(Az_M - Az_s(t)) \quad (3)$$

$$T_M(t) = T_a(t) + \frac{G_{inc}(t)}{G_{noct}}(T_{noct} - 20)\frac{9.5}{5.7 + 3.8s_w}(1 - \frac{\eta_{stc}}{af}) \quad (4)$$

$$P_{MPP}^{T_M,G^{stc}}(t) = P_{MPP}^{stc} + c_{P_{MPP}}(T_M(t) - T_a) \quad (5)$$

$$\eta^{T_M,G_{stc}}(t) = \frac{P_{MPP}^{T_M,G_{stc}}(t)}{A_M G^{stc}} \quad (6)$$

$$P_{MPP}^{25^oC,G^{inc}}(t) = FFV_{OC}^{25^oC,G^{inc}}(t)I_{SC}^{25^oC,G^{inc}}(t) \quad (7)$$

$$\eta^{25^oC,G_{inc}}(t) = \frac{P_{MPP}^{25^oC,G^{inc}}(t)}{A_M G_{inc}} \quad (8)$$

$$\eta^{PV}(t) = \eta^{25^oC,G_{inc}}(t)[1 + \frac{c_\eta}{\eta^{stc}}(T_M(t) - 25^oC] \quad (9)$$

$$P_{pv}(t) = \eta^{PV}(t)A_M G_{inc}\eta^{inv} \quad (10)$$

Equation (3) dictates the instantaneous AOI of the PV module where θ_M & Az_M the tilt angle and orientation (azimuth) of the module and θ_s & Az_s the solar elevation and azimuth, respectively. Moreover, the module's dynamic temperature T_M is dictated by the Duffie-Beckman model (4) where T_a, s_w, G_{inc}, $G_{noct} = 800W/m^2$, $T_{noct} = 44^oC$ & $af = 0.9$ the ambient temperature, the wind speed, the incident irradiance, the irradiance and temperature under normal operating conditions, and the absorptivity factor, respectively. Moreover, (5) & (6) model the effect of the module temperature on the PV power output and efficiency, while (7) & (8) dictate the related effect of irradiance.

Finally, (9) and (10) model the real module efficiency and PV power generation. In these equations, the parameters $G_{stc} = 1000W/m^2$, $P_{MPP}^{stc} = 245W$, $\eta_{stc} = 0.1943$, $A_M = 1.26\ m^2$, $c_{P_{MPP}} = -0.29\%/^oC$, $\eta^{inv} = 0.95$ & $FF = 0.788$ represent the irradiance, maximum-power-point (MPP) power, and efficiency under standard test conditions (STC), the module area, the power temperature coefficient, the efficiency of the inverter, and the module's fill factor, while the variables $V_{OC}^{25^oC,G^{inc}}$ & $I_{SC}^{25^oC,G^{inc}}$ the open-circuit (O-C) voltage and short-circuit (S-C) current of the module under the incident irradiance.

Using Monte-Carlo Simulation (MCS), 90 different winter and summer PV generation profiles were created and distributed in the DGs, varying the PV module tilt angles and orientations (tilt angle: [10°, 50°], orientation: [0°, 360°]). A weekly summer and winter PV output profiles are depicted in FIGURE 2, where it can be seen that PV generation is higher and lasts longer during Summer days.

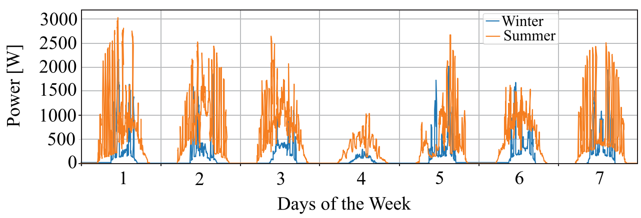

FIGURE 2. Weekly Winter and Summer PV generation profiles.

3) EV CHARGERS

The weekly profiles of the EV chargers were created using the EV driving patterns data from the Elaad open database [42], such as arrival and departure time and states of charge (SOC), requested amounts of energy, etc. The EV driving patterns and characteristics have been acquired for the following EVs: "Kona, I3, I-Pace, and Model 3" EVs with 11 kW AC-rated power, the "Model X, and Model S" EVs with 16 kW, and the "Zoe" EV with 22 kW AC-rated power. A linear approximation of the constant current (CC) and constant voltage (CV) charging regions has been considered in (11). Equation (11) dictates EV charging at constant rated current I_r until 80% SOC (CC region), and then the charging current decreases linearly to zero until 100% SOC (CV region) [43]. Moreover, a 30% consumption increase has been considered in (12) for the Winter profiles to account for higher energy consumption due to cabin heating [39], which has been integrated into the arrival SOC and requested amounts of energy of the EV fleets.

In total, 200 weekly EV charger winter and summer profiles were created for home, semi-public, and public EV chargers. As depicted in FIGURE 3, home chargers have longer parking times and requested energy amounts than semi-public/public chargers but fewer charging events [44].

$$I_{cv}(t) = 5(1 - SOC(t))I_r(t)$$
$$I_{ch}(t) = min(I_r(t), I_{cv}(t)) \tag{11}$$

$$SOC_{ar}^{win} = 1.3SOC_{ar}^{sum} - 0.3SOC_{dep}$$
$$E_r^{win} = (SOC_{dep} - SOC_{ar}^{win})B_{ev} \tag{12}$$

where: I_{cv}, I_r & I_{ch} the CV-region, rated & charging currents for every time instant t, SOC_{ar}^{win} & E_r^{win} the arrival SOC & requested energy during winter, respectively, SOC_{ar}^{sum} the arrival SOC during summer, B_{ev} the battery capacity of every EV and SOC_{dep} its departure SOC.

4) HEAT PUMPS

The HP load profiles were generated based on the heating model in [45] where a typical Dutch terraced building and an ON-OFF 3 kW-rated Dimplex LIK 8MER have been used as building and HP models, respectively. In addition, the required inputs are the building and HP specifications, weather data from Metenorm, and residential/commercial occupancy profiles. The heating model has developed the HP load profiles by keeping the building temperature T_b within the desired limits [21° C, 23° C] using floor-heating and is summarized in the following equations.

$$T_b(t + \Delta t) = \frac{\dot{Q}_{hp}(t) + \dot{Q}_{ir}(t) - \dot{Q}_{los}(t)}{C_b + V_b C_{air} \rho_{air}} \Delta t + T_b(t) \tag{13}$$

where:

$$\dot{Q}_{los}(t) = \dot{Q}_{cond}(t) + \dot{Q}_{vent}(t) \tag{14}$$

$$P_{hp}(t) = \frac{\dot{Q}_{hp}(t)}{COP(t)} \tag{15}$$

$$COP(t) = 7.90471\ e^{-0.024(T_{ret}(t) - T_a)} \tag{16}$$

$$T_{ret}(t) = T_{sup} - \frac{\dot{Q}_{hp}(t)}{\dot{m}_{wat} C_{wat}} \tag{17}$$

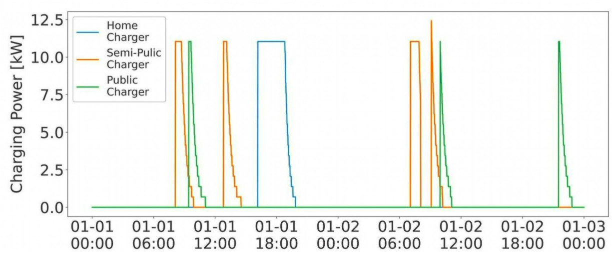

FIGURE 3. Home, Semi-public & Public Charger Profiles for 2-days Simulation.

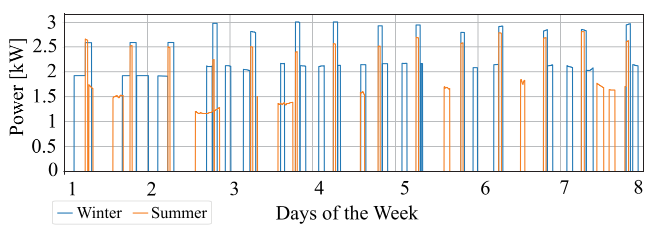

FIGURE 4. Weekly Winter and Summer HP profiles for the residential buildings.

The temperature dynamics are dictated in (13) and depend on the $\dot{Q}_{hp}$, $\dot{Q}_{ir}$, $\dot{Q}_{los}$ which represent the HP output, heatings gains by incident irradiation and heating losses, respectively, divided by the total building thermal capacity (the thermal capacity of the building structure $C_b = 4.755\ kWh/K$ and of the encapsulated air volume $V_b = 585\ m^3$). Additionally, the total losses $\dot{Q}_{los}$ comprise the conductive losses $\dot{Q}_{cond}$ & ventilation losses $\dot{Q}_{vent}$ in (14). Moreover, a water tank is heated twice daily, at 06:00 and 19:00, for domestic hot water (DHW) use. The HP power consumption has been calculated as dictated in (15), where COP is the HP Coefficient of Performance and is modeled in (16). Finally, the COP depends on the HP return water temperature T_{ret} dictated in (17) where $\dot{m}_{wat} = 0.8\ kg/s$ & $C_{wat} = 1.16\ Wh/kgK$ the flow water rate and the water specific capacity, respectively, and T_{sup} the supply water temperature set at 35°, 50° and 18° for floor-heating, DHW and floor-cooling.

The weekday occupation profiles have been considered to be outside the window [08:00, 14:00] for the residential buildings and between [09:00. 21:00] for the commercial ones. During the weekends, the residential buildings have been assumed to be always occupied while the commercial buildings are occupied between 09:00 and 18:00. Using normal distribution for the occupation and disoccupation building times, 200 winter and summer weekly profiles have been created for the residential and commercial buildings. FIGURE 4 depicts weekly winter and summer HP consumption profiles for a residential building where the high peaks belong to DHW use and the low peaks belong to floor heating/cooling.

C. SEASONAL ANALYSIS OF LCT POWER PROFILES

In FIGURE 5, power profiles for PVs, HPs, and EVs during Winter (upper row) and Summer (lower row) are summarized so that the seasonal differences of the LCTs are further clarified. Concerning PVs, PV power is generated between [09:00 and 16:00], with the highest power peak of 2.5kW occurring at 12:00. In contrast, PV generation lasts longer during Summer (more specifically between [05:00, 20:00]), having higher power peaks that reach up to 3.2kW. A weekly average PV rooftop generation is approximately 132kWh during Winter and 281kWh during Summer (113% higher).

Moreover, regarding the ON-OFF HPs, the high pulses belong to DHW while the low pulses to space heating and cooling in Winter and Summer, respectively. During Winter, building heating is performed with approximately 2kW HP power, while building cooling needs only 1.5-1.6kW power. This is justified by the more moderate difference between the ambient and building temperatures, since the building temperature is maintained between [21° C), 23° C)], and the ambient temperature deviates between [20° C), 30° C)] and [−5° C), 10° C)] during Summer and Winter, respectively. Furthermore, building cooling in Summer occurs mostly in the afternoon and endures approximately 4h, while building heating in Winter occurs in the night and in the evening and lasts approximately 8h (100% longer than cooling). The seasonal difference in DHW power consumption is lower due to the high supply temperature for DHW (50° C); however, the time needed for water heating in Winter is considerably higher. A weekly average HP energy consumption is approximately 286kWh during Summer and 645kWh during Winter (126% higher). Finally, it can be seen that HP consumption for cooling is more likely to overlap with PV rooftop generation during Summer than HP consumption for heating during Winter.

Finally, the 30% higher EV consumption (hence, requested energy) during Winter due to cabin heating is visible in FIGURE 5 c), since the EVs arrive with a lower SOC than in FIGURE 5 f). While the power levels remain unchanged,

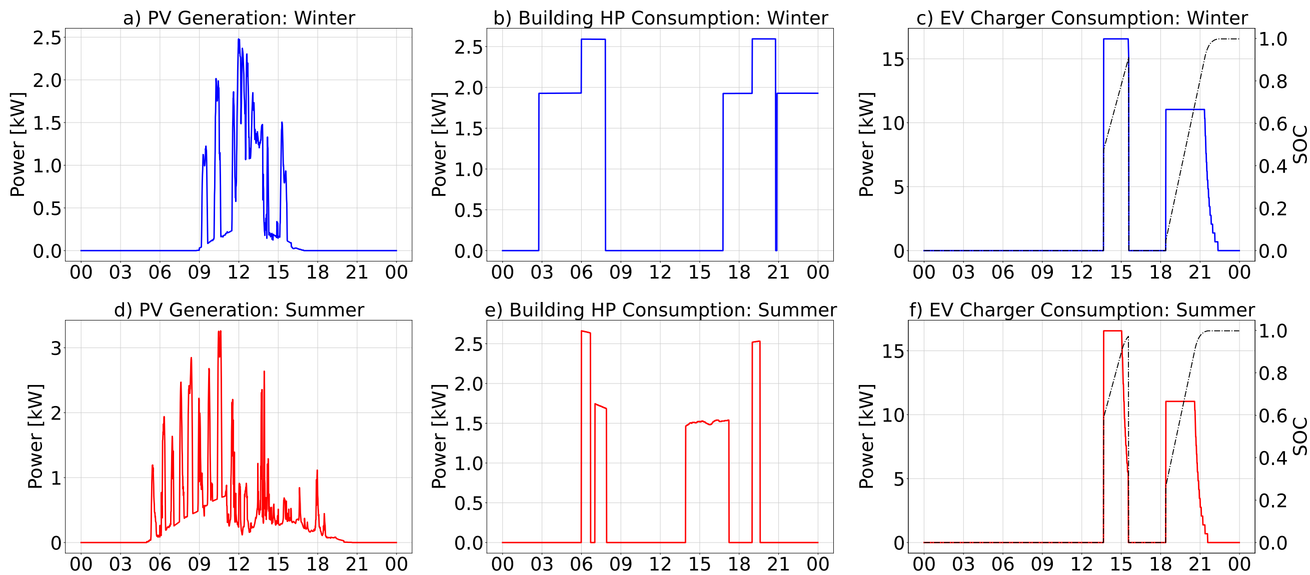

FIGURE 5. Daily Power Profiles for PVs, HPs, and EVs during Winter [a), b), c)] and Summer [d), e), f)].

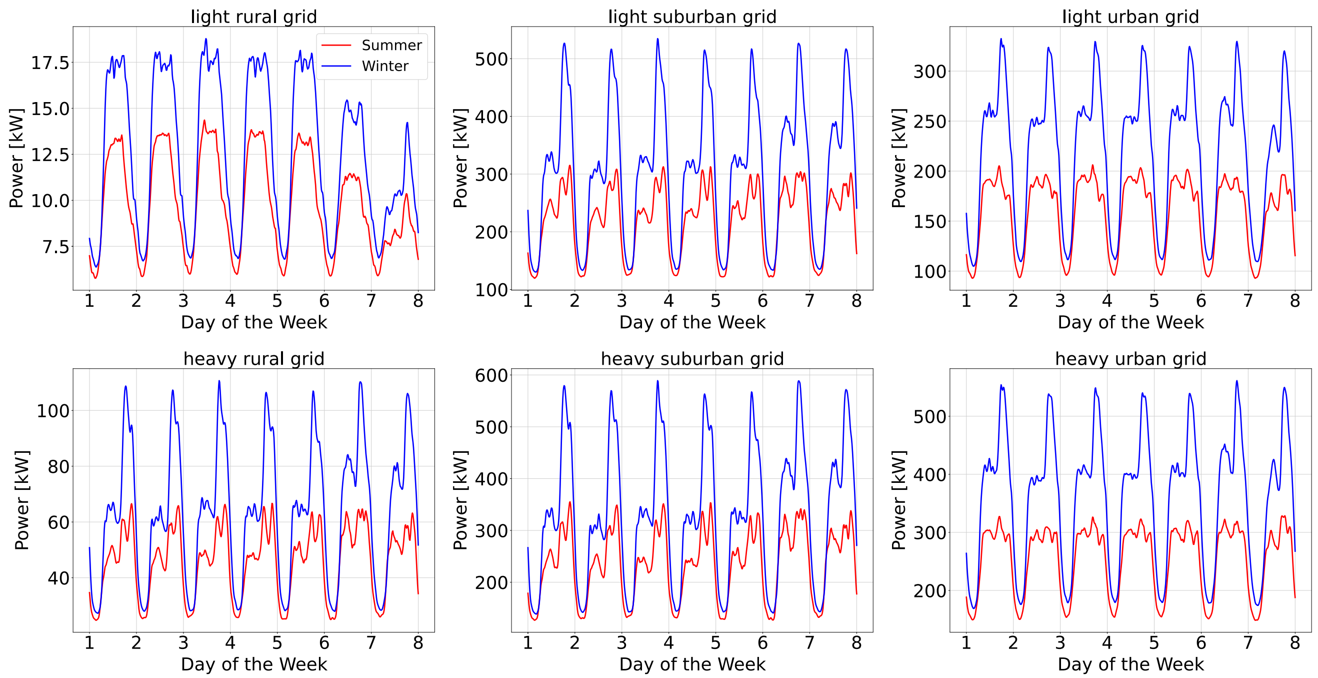

FIGURE 6. Existing loading profiles of the six LV DGs during Summer and Winter.

since the EVs are charged with the rated charging power in uncontrolled charging, the total charging duration can considerably increase (e.g. 30-45' longer).

D. LOAD AND LCT PHASE CONNECTIONS

In this work's unbalanced simulations, two-phase connection types were considered according to each LCT specification: three-phase WYE connections and single-phase-to-neutral connections, which can be connected to any phase.

1) PHASE CONNECTION OF BASE LOAD

The phase connections of the base load depend on the building specifications, which were provided together with the DGs provided by Enexis groep.

2) PHASE CONNECTION OF HEAT PUMPS AND PV SYSTEMS

Both HP and PV systems are distributed as single-phase components since both LCTs have a 3 kW rated power level, which is below the legal limit for single-phase components [7]. When an HP or PV system is assigned to a single-phase connected building, the LCT is connected to the same phase as the building. In the case of a three-phase connected building, the LCT is connected randomly to the one phase.

3) PHASE CONNECTION OF EV CHARGERS

Regarding the EV chargers, the number of EV charging phases depends on the rated power levels of the incoming EVs. A 7.4 kW-rated power constitutes the maximum limit for single-phase EV charging, which relates to a maximum 32A phase current at a 230V node voltage. The charging of EVs that have a higher rated power (11-22 kW) is realized using all three phases. It must be noted that most EV driving patterns have rated charging powers above 7.4 kW (11 kW, 16 kW, or 22 kW). Hence, to allow simulations with both single- and three-phase charging, the rated charging power of all 11 kW-rated and of 50% of the 16 kW-rated EVs has been reduced to 7.4 kW, increasing the charging time window and keeping the requested energy the same. The charging of the rest of the EVs (50% of the 16 kW-rated and all 22 kW-rated) was performed three-phase.

IV. LV GRIDS, LCT GRID DISTRIBUTION, CASE STUDIES, AND SIMULATION SET-UP

A. LV GRIDS

The investigation is conducted on six Dutch LV distribution grids (DGs) [43], which are provided by Enexis [46]. The grids are divided into light- and heavy-loaded rural, suburban, and urban distribution grids. Each provided LV grid is connected to the main grid via an MV/LV transformer and integrates loads corresponding to residential or commercial buildings, which were provided with associated data, such as yearly consumption, phase connections, maximum phase currents, etc. With the use of each load's yearly consumption E^i, the distribution profiles $P_d(t)$ from [38] and (2) (see Section III-B.1), the load consumption profiles were generated and integrated into the grids. Similarly, the generated profiles of LCTs such as PV systems, EV chargers, and heat pumps from Sections III-B.2-4. were integrated into the grids depending on the number and type of buildings/loads and LCT combinations and penetrations described later in Section IV-B. to investigate the effect of phase unbalance in the DGs.

It must be noted that the LCT profiles were integrated with a similar manner into the light- and heavy-loaded grids which are independent from the size of the grids or the grid buildings and depend only on the phase connections and LCT grid distribution methodology described in Sections III-D. and IV.C, respectively. Hence, the generation of the LCT profiles was realized only with the use of specific real PV, EV, and HP modules and the models described in Section III-B. Moreover, the number of the integrated LCTs into each grid depends only on the number of the grid loads; hence, a heavy-loaded grid integrates a higher number of LCTs than its light-loaded counterpart under the same penetration due to a higher number of existing loads. The methodology of LCT grid distribution for each grid and case study is thoroughly described in Section IV-C. Finally, the most important characteristics of the 6 LV grids are summarized in FIGURE 6 and TABLE 2 to show the differences between the light- and heavy-loaded grids of the same type.

FIGURE 6 depicts the existing loading of the six LV grids with 0% LCT penetration during Winter and Summer weeks. It can be seen that the Winter base load is always higher than the respective Summer load. Moreover, comparing the same grid types, the load power peaks can be considerably higher in the heavier-loaded grids which can reach up to 6x and 1.5x times higher in the rural, and urban grids, respectively. This can be also seen in TABLE 2 which summarizes the number of buildings and nodes and the yearly consumption in MWh for each investigated grid. Finally, the grids are depicted in FIGURE 7.

TABLE 2. Characteristics of the 6 LV distribution grids.

Grid	Buildings	Nodes	Yearly Consumption
Light Rural	3	28	97,954 MWh
Heavy Rural	138	546	486,782 MWh
Light Suburban	266	873	2353,034 MWh
Heavy Suburban	480	1419	2830,574 MWh
Light Urban	123	339	1680,223 MWh
Heavy Urban	296	1512	2745,560 MWh

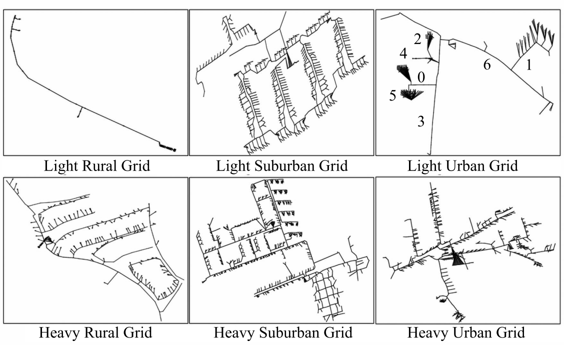

FIGURE 7. 6 Dutch LV Distribution Grids (Enexis Groep).

B. CASE STUDIES

The case studies of this work have been summarized in TABLE 3. As explained, 6 DGs have been utilized, one light- and one heavy-loaded grid per rural, suburban, and urban category, to account for the grid type and existing grid loading influences on phase unbalance. Moreover, 3 LCT combinations have been considered to study the interrelated unbalance impact of PV integration with EV, HP, and EV-HP integration in the DGs under 4 increasing penetrations (0, 50, 80, 100%).

Finally, 4 main unbalance factors are considered: the LCT phase connections, grid locations, Summer and Winter seasons, and LCT power- and consumption-levels. The fourth unbalance factor has also been evaluated as a potential mitigation measure, utilizing average charging (power-based measure) and thermal comfort decrease (consumption-based measure) for EVs and HPs, respectively.

C. LCT GRID DISTRIBUTION

With the use of the developed LCT models of Section III-B., a pool of PV, EV, and HP profiles has been generated. From the 3 respective pools, LCT profiles have been randomly selected, using the normal distribution, and distributed to the 6 LV DGs according to each penetration and combination case study. An example of the LCT grid distribution is shown in FIGURE 8 for the heavy rural grid. The LCT penetration level depends mainly on the number of buildings (existing loads). FIGURE 8 a. depicts the heavy rural grid with the existing loads without LCT penetration. A penetration of 50% means that half of the buildings comprise a PV rooftop, an HP module, and an EV charger (see FIGURE 8 d. where a part of the grid is depicted). Moreover, the LCTs have been randomly distributed independently. Hence, a building may comprise a PV rooftop and not an HP or EV.

In continuation, 80% and 100% LCT penetration levels are depicted in FIGURE 8 e. and f. The LCT profiles have been increasingly added to the DGs under the increasing penetrations, meaning that all buildings that comprised, e.g., a PV rooftop at 50% penetration, will comprise a PV rooftop also at 80% penetration. Hence, every next penetration level comprises the LCTs of the previous level at the exact locations. Furthermore, a penetration of 100% means that all buildings comprise one of all 3 LCTs. Finally, PV systems and HPs have been distributed to the existing buildings, regardless of their type (residential or commercial). In contrast, home EV chargers have been distributed at the residential buildings while public and semi-public EV chargers have been distributed at the commercial buildings. No LCT of the same type could be connected to the same node.

D. SIMULATION ENVIRONMENT AND SET-UP

The simulation period has been selected to be one week to capture the intra-weekly effects. For example, the occupations of residential and commercial buildings differ

TABLE 3. Case studies for LCT impact on phase unbalance.

Case Studies				
Distribution Grids	LCT Combinations	LCT penetrations	LCT Unbalance Factors	Mitigation Measures
2 Rural (light & heavy)	PVs-EVs	0 %	1. LCT phase connections	1. EVs: Average charging (power-based measure)
2 Suburban (light & heavy)	PVs-HPs	50 %	2. LCT grid locations	2. HPs: thermal comfort decrease (consumption-based measure)
2 Urban (light & heavy)	PVs-EVs-HPs	80 %	3. Seasons: Winter & Summer	
		100 %	4. LCT power & consumption levels **(evaluated and as mitigation measures)**	

during weekdays and weekends. Moreover, the amount of EV charging events also differs during the week [42]. Furthermore, the timestep of the simulation has been set to be 1 minute to realize a trade-off between accuracy and computational time. The most computationally expensive simulations (for the heavy suburban grid) remained under 90 minutes, which is considered appropriate for grid scheduling unbalance studies. Moreover, 1-minute simulations can more accurately consider the coincidence factor of LCT operation [47]. Finally, the AC-unbalanced Newton-Raphson load flow calculation method was utilized for the unbalance analysis of all investigated grids, LCT combinations and penetration levels. The grid simulations were realized in the DigSilent PowerFactory 2019 environment, while the LCT integration management was performed in the Python 3.9 environment.

V. RESULTS

A. PHASE CONNECTIONS: UNBALANCE FACTOR (UF) 1

1) INTRODUCTION OF PHASE CONNECTIONS

Firstly, the phase unbalance was studied by randomizing the LCT phase connections at their initial locations, which were obtained from [39] to compare the results with the related results of the balanced integrations and to be used as a base case study. A uniform probability function in a Python environment was used to randomly select the integrated LCT profiles from their respective families.

2) PHASE CONNECTIONS-RESULTS (1): UNBALANCE MAGNITUDE AND DURATION

FIGURE 9 depicts the maximum and average VUF in the 6 DGs for 0%, 50%, 80% & 100% LCT penetration levels and all LCT combinations after randomizing their phase connections. No phase unbalance is seen in the light rural grid under any circumstances. For the urban grids and the heavy rural grid, the maximum unbalance is below 3%. The heavy suburban grid exceeds 3% for 80% and 100% LCT penetration even for the PV-HP scenario, reaching a maximum VUF of 7.5%, whereas in the light suburban grid, the VUF overpasses slightly the threshold of 3% at 50% and 100% combined penetration levels.

These observations show that voltage unbalance depends heavily on the type of grid and the existing grid loading conditions summarized in TABLE 2, and it generally increases with higher LCT penetrations. For example, the light-loaded rural grid maintains low voltage unbalance for all levels of LCT penetration. Even for 100% penetration, the maximum VUF stays below 0.35%. However, the heavy rural grid reaches a maximum of 1.6% unbalance at 100% combined LCT penetration, five times higher than the light counterpart. Similar observations have been made for all depicted light and heavy suburban grid scenarios.

Moreover, the significant influence of the existing grid loading can be seen not only by comparing the unbalance inflicted by the same LCT combinations on different DGs but also by comparing the combined PV-EV-HP integration with the partial PV-EV and PV-HP integrations in the same DG. It can be seen that in the suburban grids that are already characterized by higher existing loading than the rural and urban grids, the combined PV-EV-HP can increase voltage unbalance by a factor up to 100% compared to the PV-EV and PV-HP integrations which are not seen in the other types of grids.

However, a decrease of unbalance in increasing penetration levels can also be seen in several cases, e.g., from 50% to 80% penetration for the light suburban grid or from 80% to 100% for the light urban grid. This is justified because integrated LCTs at higher penetration levels can even out LCTs at lower levels if the extra load is added to a different phase (or extra generation is added to a phase with existing loads).

Regarding LCT comparison, the highest VUF was observed for the PV-EV-HP integration scenario, as expected for all grids. However, for almost all grids and LCT penetration levels, voltage unbalance is higher for HP integration than for EV chargers. Especially for both the light rural and heavy urban grids, it can be seen that the unbalance in the PV-HP-EV integration scenario is very close to the unbalance in the PV-HP scenario. This can be justified, firstly, by the fact that HP operation lasts longer than the fewer EV charging events to continuously maintain the building's thermal comfort, as seen in FIGURES 3, 4. Secondly, all HPs are single-phase LCTs due to low power rating while multiple EV charging sessions are realized with $> 7.5kW$ charging power and use all 3 phases for EV charging.

As the Dutch electricity code obligates DSOs to maintain a VUF lower than 3% for 95% of the time at the point of

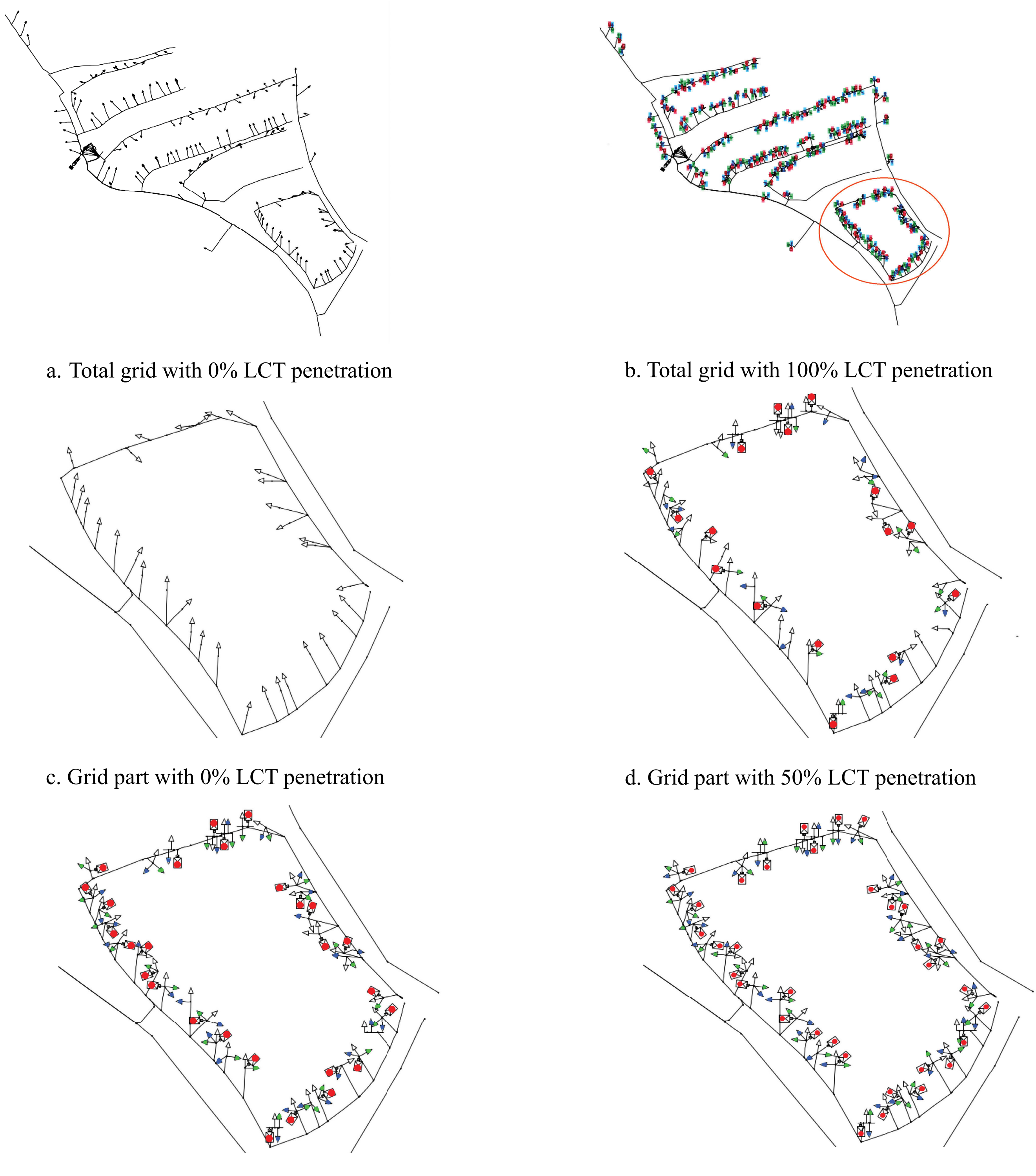

a. Total grid with 0% LCT penetration

b. Total grid with 100% LCT penetration

c. Grid part with 0% LCT penetration

d. Grid part with 50% LCT penetration

e. Grid part with 80% LCT penetration

f. Grid part with 100% LCT penetration

FIGURE 8. LCT grid integration in the heavy-loaded rural grid under 0, 50, 80, and 100% LCT penetrations: Red color (PVs), Blue color (EVs), Green color (HPs), Black color (existing loads).

common coupling [7], the duration of unbalance exceeding certain levels was investigated. The hourly duration of 0.5, 1, 2 & 3% VUF that every grid experiences for 100% combined LCT penetrations is depicted in FIGURE 10. The heavy-loaded grids experience more long-lasting voltage unbalance than their lighter counterparts. While the light rural grid experiences no unbalance, the heavy rural grid is characterized by a VUF > 0.5% for more than 6 hours during

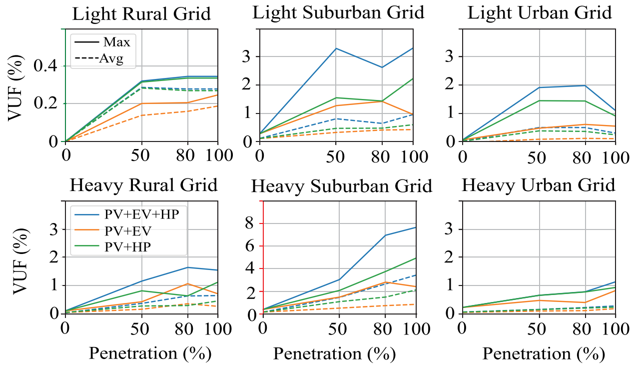

FIGURE 9. Maximum and average VUF in the 6 DGs for all LCT penetration levels and combinations in the initial locations.

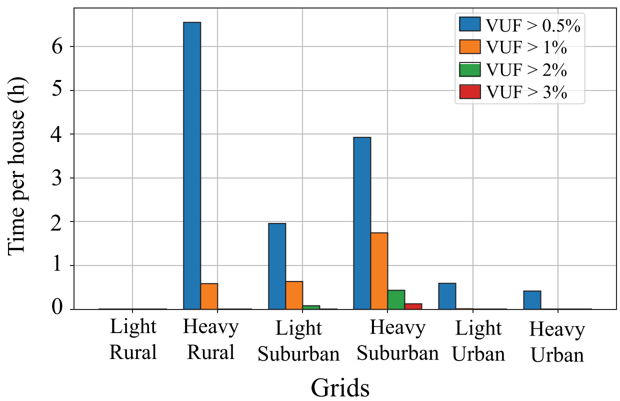

FIGURE 10. Duration of maximum VUF exceeding certain levels for 100% PV, EV & HP penetration.

the week. However, VUF remains under 1%. The heaviest voltage unbalance of the heavy suburban grid is also seen here, which is the only grid exceeding 3%.

3) PHASE CONNECTIONS-RESULTS (2): GRID COMPARISON

In FIGURES 9 & 10, it is observed that in contrast with the rural and suburban grids, the light urban grid shows a slightly higher unbalance than the heavy one such concerning magnitude (more than double for 50% and 80% penetrations) as also concerning duration. Therefore, the investigation proceeded to grid analysis to justify this observation.

FIGURE 11 depicts the amount of energy consumption in the 6 DGs regarding the distance from the MV/LV transformer (T/F) that connects the DG with the main grid. Moreover, FIGURE 12 visualizes the relative distance (0-1) at which 50% of the total feeder energy is consumed inside the radial feeders in the grids to show which feeders are more heavily loaded at their first or their second half. In this regard, nearly all consumption occurs at the furthest point of the loaded feeders of the light urban grid, apart from feeders 3 and 4, which are empty. This can also be seen for the light urban grid in FIGURE 7, which depicts the grids' spatial visualizations. In contrast, 50% energy consumption occurs at around 60%-80% feeder length in most of the radial feeders of the heavy-loaded urban grid. Hence, consumption at longer distances from the T/F contributes to the increase of unbalance (heavy suburban grid). However, the distance inside the radial feeders has an equally significant effect.

Moreover, information about the percentage of loads situated at radial feeders is provided in TABLE 4 to strengthen the above conclusion. The rural and urban grids consist only of radial feeders, while the suburban grids service loads through a combination of meshed and radial feeders, as can also be seen in FIGURE 7. It is also seen here that 100% of the loads in the light urban grid are placed in radial feeders.

The reasoning for the effect of distance on unbalance in the radial feeders comes from the fact that voltage deviations are more severe when higher consumption occurs at the end of the feeders due to the higher impedance in the distribution line. Additional randomly phase-connected loads that simultaneously draw power from different phases can provoke a higher phase unbalance at distant nodes, which are characterized by a higher voltage drop.

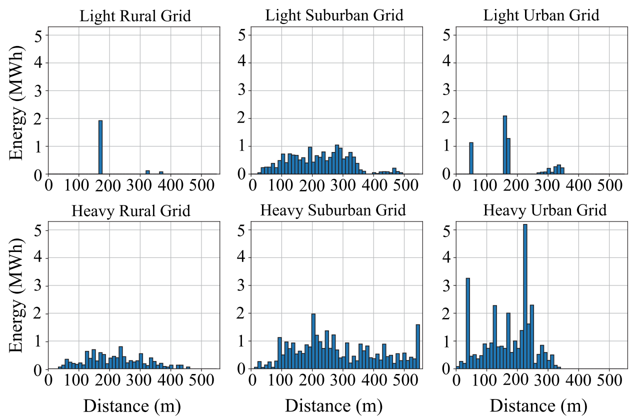

FIGURE 11. Energy Consumption amount at the distance from the MV/LV Transformer of the distribution grids.

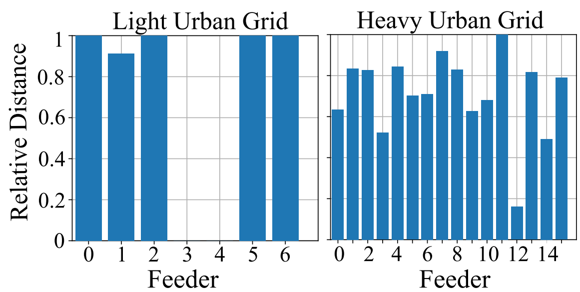

FIGURE 12. Relative feeder-length point that 50% energy consumption occurs at the radial urban grids' feeders.

B. LCT GRID LOCATIONS: UNBALANCE FACTOR 2

1) INTRODUCTION AND CONTRIBUTION OF LCT GRID LOCATIONS

Secondly, after the unbalance impact analysis of random LCT phase distribution, the work proceeded to study the effect of LCT grid distribution. In this regard, 10 different LCT distributions were simulated for each of the 0, 50 & 100%

TABLE 4. The load share per grid in radial feeders.

Grid	% Loads in feeders
Light Rural	100%
Heavy Rural	97.8%
Light Suburban	19.5%
Heavy Suburban	78.3%
Light Urban	100%
Heavy Urban	99.7%

penetration levels in order to show the effect of the LCT locations, which has not yet been studied for different real-world grid case studies (rural, suburban, urban). For each of the 10 iterations, the LCTs were also here increasingly inserted in the DGs according to the increasing penetration levels, meaning that every next penetration level comprises the LCTs of the previous penetration level in their previous grid locations.

2) LCT GRID LOCATIONS-RESULTS

The maximum VUF results of the above iterations for all DGs and LCT combinations are presented in FIGURE 13. Similar to the results of the previous section, the light rural grid maintains the lowest voltage unbalance, while the heavy suburban grid experiences the highest voltage unbalance. Irrespective of the LCTs used, the median maximum VUF increases for increasing LCT penetration. Moreover, the unbalance in the PV-EV-HP scenarios is closer to the unbalance in the respective PV-HP scenarios in most grids. Hence, the previous observation that EV integration has a smaller impact on the unbalance than HP integration is also strengthened here and is irrespective of the LCT locations. In addition, the light urban grid suffers from an equal or slightly higher unbalance than the heavy urban grid despite its lower amount of loads, as also expected from our previous grid analysis. Finally, the already highly loaded suburban grids present a much higher VUF during combined PV-EV-HP integration (up to 300% increase compared to the other two partial combinations), an observation that was also made in FIGURE 9.

Furthermore, it is also observed that the phase unbalance variance is higher in the light-loaded grids than in their heavy-loaded counterparts. This can be justified by the fewer amount of loads and LCTs in these grids that affect more significantly the unbalance results according to their location in the grid feeders. On the contrary, a random re-distribution of a vast amount of loads at the nodes of a DG changes more moderately the status quo of the grid situation. This can be seen especially for the light rural grid, which, with a median maximum VUF of 0.48% at 50% PV-EV-HP penetration, is characterized by a variance of approximately 0.2%. Hence, it can be concluded that the unbalance factor of LCT grid distribution is less impactful than expected. This is justified by the fact that all our insights from Section V-A. concerning the comparison of different DGs, LCT combinations, and penetrations remain the same, and the most notable impact has been on the variance of the VUF results regarding the grid type and loading.

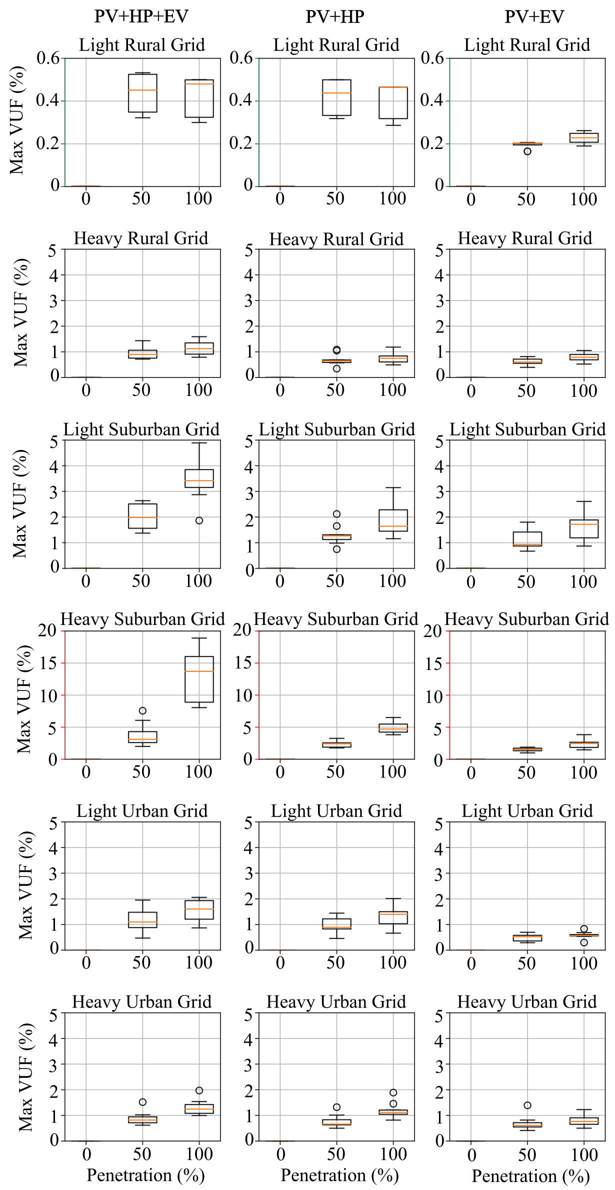

FIGURE 13. Maximum grid VUF for 10 iterations of randomized LCT locations for PV-HP/PV-EV/PV-HP-EV combinations under 0%, 50% & 100% penetrations.

Regarding further comparison between EV and HP integration, FIGURE 14 depicts the median VUF of the PV-EV and PV-HP 100% integration scenarios against the median VUF of the 100% PV-HP-EV integration scenario for all DGs. The interpretation of the figure is that the distance of the VUF markers of the one combination in the Y axis (e.g. PV-HP) from the dashed grey identity line depends on the influence of the other combination (e.g. PV-EV) and vice versa, as compared with the PV-EV-HP combination in the X axis. Hence, if the influence of the PV-EV integration were negligible, the markers of the PV-HP scenario would lie on the identity line. Therefore, the vertical distance to the identity line can be interpreted as the impact of the omitted LCT. For most of the grids, the PV-HP integration VUF markers are closer to the identity line, indicating that the impact of EVs on unbalance is notably lower. For the heavy suburban grid, the outliers suggest that they contribute greatly in combination.

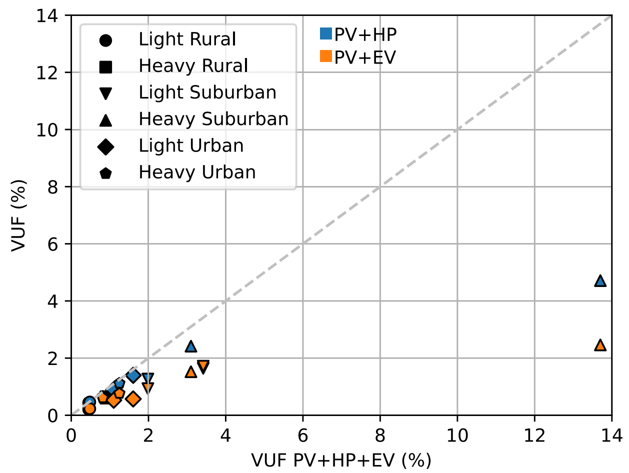

FIGURE 14. The median VUF of the different scenarios (PV+HP and PV+EV) plotted versus the median VUF of the scenario PV+HP+EV under 100% penetration.

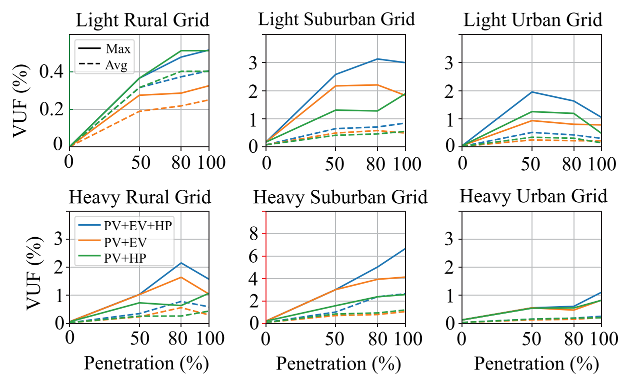

FIGURE 15. Maximum and average VUF for 0, 50, 80 & 100% penetration of PV-EV, PV-HP & PV-EV-HP LCT combinations during Summer.

C. SEASONS: UNBALANCE FACTOR 3

1) INTRODUCTION AND CONTRIBUTION OF SEASONS

Thirdly, the focus has been placed on showing the effect of different seasons on the unbalance impact of LCT integration. As already shown in Section II-C., an unbalance impact comparison due to the integration of different LCT combinations under different seasons, e.g. Summer and Winter, is still missing from the existing works that comprise PVs, EVs, and HPs. More specifically, this work has already conducted a comparative analysis of EVs and HPs in different PV-integrated grids during Winter in Sections V-A. & VB. However, the seasonal effect has a strong influence on the profiles of all 3 LCTs since, on the one hand, the PV generation highly increases in Summer, and on the other hand, the EV and HP consumption highly increase in Winter.

Hence, the Summer season can alter significantly the Winter findings by the comparative unbalance assessment due to the combined integration of PVs-EVs and PVs-HPs. For this case study, in order to avoid the effect of the LCT phase and grid distributions, the LCTs were distributed again back to their initial grid locations and phases for a fair comparison with the respective winter results in FIGURE 9.

2) SEASONS-RESULTS

FIGURE 15 shows the maximum and average voltage unbalance during a Summer week for the considered LCT combinations, penetration levels, and DGs. Regarding the combined PV-EV-HP integration scenarios, a slightly lower unbalance can be seen during Summer for most of the grids. For example, the maximum VUFs for the light and heavy suburban and urban grids for the Winter season are 3.2, 7.8, 1.1 & 1.1%, respectively, while the respective numbers for the Summer season are 3, 6.2, 1 & 1%. However, the PV-EV integration produces similar or higher unbalance than PV-HP integration in most penetrations apart from the light rural and urban grids. The reasoning behind this difference is twofold. Firstly, the HP consumption decreases significantly during Summer, especially for the Dutch grid case studies, which are characterized by a more moderate ambient temperature. This is also concluded in [45] for which the same LCT profiles were utilized. Hence, PV-HP integration scenarios result in lower unbalance than in the Winter season. EV consumption also decreases due to the lack of cabin heating. However, this decrease amounts to 30% while HP heating consumes approximately 50% more energy than HP cooling.

Secondly, PV generation is assumed to be integrated into all the simulated scenarios. PV generation coincidences for a higher duration with EV charging than HP cooling because the buildings are mostly unoccupied when PV power is generated since most of them are residential. Concerning balanced power flows, coincident LCT operation is mostly beneficial for better grid impact mitigation. However, it can become detrimental for unbalanced power flows if LCTs inject and withdraw power from different phases simultaneously, increasing phase unbalance. Therefore, considering also the higher PV generation during Summer (see FIGURE 2), and hence higher phase power difference, PV-EV integration scenarios result in higher unbalance compared to Winter.

D. LCT CONSUMPTION AND POWER LEVELS: UNBALANCE FACTOR 4

1) INTRODUCTION AND CONTRIBUTION OF LCT CONSUMPTION AND POWER LEVELS

Finally, the LCT power and consumption levels have been studied as final phase unbalance factors for EV chargers and HPs, respectively. This part was realized for different LCT locations and 0%, 50% & 100% penetration levels, however, only for the Winter season. The maximum and mean VUF metrics were utilized for the unbalance analysis since they are correlated with the impact of the peak power and consumption on unbalance, respectively.

Averaged EV charging has been used to study the effect of power levels on voltage unbalance inflicted by EV grid integration. In averaged charging, the power levels are decreased since the charging power is averaged over the parking time of each vehicle for all EV charger profiles while keeping the energy consumption the same [48]. This is shown in (18) where P_{ch}, E_r, T_p the charging power, requested energy, and parking time, respectively. It must be noted that the CV charging region was not considered in the average charging.

$$P_{ch}(t) = E_r/T_p \tag{18}$$

On the contrary, the HP consumption levels have been lowered with a slight decrease in the building thermal comfort to study the effect of the LCT consumption levels on voltage unbalance inflicted by HP integration. This was realized by decreasing the desired temperature interval from [21°C, 23°C] to [20°C, 21°C] in the HP heating model presented in Section III-B.4. Hence, new lower-consumption HP heating profiles were generated and distributed in the initial phases and locations of Section V-A. for the Winter season to cancel out the effect of the other unbalance factors. While average EV charging affects the LCT power levels, decreasing the desired building temperature affects the LCT consumption levels. This is because while it decreases the total HP consumption needed to keep the thermal comfort of the buildings, the power levels are hardly changed since the utilized HPs are ON-OFF and not variable-speed. Moreover, since the unbalance factor was tested for the Winter season, the desired temperatures have been decreased to reduce the heating consumption. To apply the concept during Summer, the desired temperatures should be increased to reduce the HP cooling consumption.

2) LCT CONSUMPTION AND POWER LEVELS-RESULTS

This case studies the effect of different power and consumption levels of the integrated LCTs on voltage unbalance. This case ("Low Power Mode" in FIGURE 16) has been investigated only for Winter and three distribution grids: light- and heavy-loaded urban grids and the heavy-loaded suburban grid. FIGURE 16 depicts the VUF magnitude results of the "low power mode" on the right with the original results (named as "normal") on the left, which are taken by FIGURE 9. Moreover, FIGURE 17 shows the respective comparison concerning the duration of unbalance with VUF above certain levels at 100% PV-EV-HP penetration.

Varying power and consumption levels for EV charging and HP heating, respectively, has varying effects on the VUF violation magnitude and duration. On the one hand, the duration of the unbalance is decreased for all DGs in a range between 11% and 25% regarding all VUF levels, as seen in FIGURE 17. On the other hand, the effect on the VUF magnitude varies per combination. Concerning, the PV-HP integration scenarios, a lower VUF can be seen (up to 15% decrease) regarding both maximum and average VUF when the HP consumption levels are decreased. However, concerning the PV-EV integration scenarios, an approximate 60% VUF increase is observed in the light urban grid (VUF reached 0.8% from 0.5%) while a 30% decrease is seen in the heavy urban grid, both at 100% penetration level. Moreover, a VUF increase of 20% is observed for the combined PV-EV-HP scenario at 100% penetration level at the heavy suburban grid (VUF reached 10% from 8%).

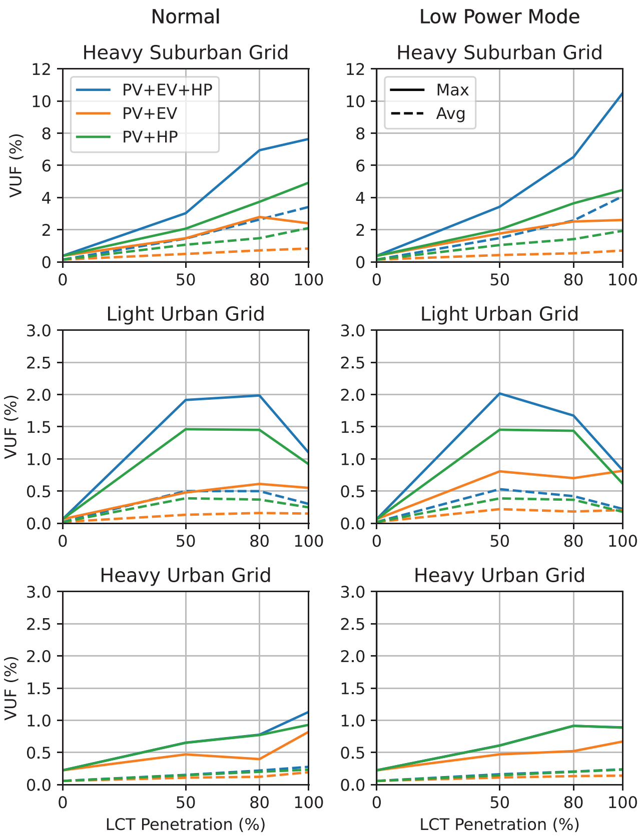

FIGURE 16. Comparison of average and maximum VUF produced by the low and original power modes for all LCT combinations and penetrations in 3 DGs.

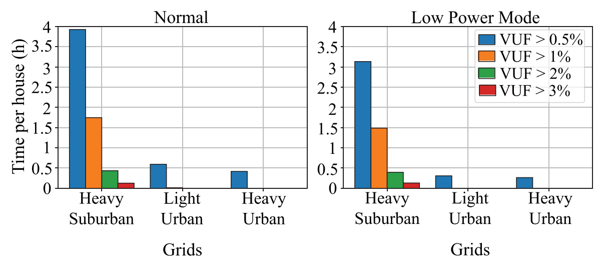

FIGURE 17. Comparison of the duration of the maximum VUF produced by the low and original power modes for 100% PV-EV-HP penetration.

As discussed, this case study has different effects on HP operation and EV charging. While energy consumption for HP heating is decreased due to lower thermal comfort, the effect on the power peaks of the ON-OFF HP operation is minimal. This is because while the ON HP duration is decreased, the power peak itself remains the same since it depends on the COP and the ambient temperature. On the contrary, average EV charging results in the following opposite effects. While the power peaks of EV charging are reduced, the duration of the EV charging is increased since the EV is charged during the whole parking time because the total amount of requested energy remains the same. Hence, on the one hand, simultaneous PV peak power injections and EV peak power withdrawals during uncontrolled charging (normal mode) can result either in a higher VUF if they occur on different phases or in a lower one if they occur on the same. On the other hand, the prolonged EV average charging (low power mode) can reduce the VUF due to reduced power peaks but also increase the probability of a higher VUF in time due to increased simultaneous operation with the PVs. Therefore, it can result in contradictory observations. For example, a lower maximum VUF is observed at 80% penetration of the combined PV-EV-HP integration in the heavy suburban grid (6.1% instead of 7%) during the mitigation mode, whereas VUF increase is noted at 100% penetration (10.1% instead of 7.9%).

E. EVALUATION OF LCT CONSUMPTION AND POWER LEVELS VARIATION AS PHASE UNBALANCE MITIGATION MEASURES

This work evaluates varying the LCT consumption and power levels as a potential unbalance mitigation measure for HPs and EVs, respectively. The reasoning behind the investigation of such strategies is, firstly, their simplicity in implementation and, secondly, the potential of mitigation without the installation of further assets, such as ESSs. Such unbalance mitigation measures were only investigated in [27]; however, only for EVs and the study did not consider HP integration.

While simple, the two implemented control strategies managed to have some notable effects on voltage unbalance mitigation. Firstly, the duration of VUF violation was decreased up to 25% for all investigated distribution grids, which is especially important for the heavy-loaded suburban grid, which suffers from the highest voltage unbalance levels. Secondly, decreasing the LCT consumption levels could effectively decrease the voltage unbalance up to 15%, although the mitigation measure was not effective enough to reduce the VUF of the heavy suburban grid below the 3% legal limit. Finally, decreasing the LCT power levels at expense of consumption duration was found to have uncertain results concerning voltage unbalance mitigation; while the VUF will be decreased during the previous charging window, it can be increased during the extended window when the operation of PVs and EVs overlap in different phases. This is also the reason why the VUF magnitude could result in higher or lower; however, the duration of the violation is always decreased. Hence, it can be seen that while peak power levels are important for phase unbalance decrease, the consumption duration is also significant. A mitigation measure that affects both should be implemented only with coordination of the phase connections of the LCTs. For example, the PVs and EVs must inject and withdraw power, respectively, to and from the same phase.

Overall, this work was mainly devoted to quantifying the voltage unbalance impact by the grid integration of PVs, EVs, and HPs, addressing different combinations, penetration levels, and influencing factors. Additionally, the work proceeded to evaluate the fourth unbalance factor as a mitigation measure due to its simplicity and lack of need for additional assets and investments. It has effectively reduced the voltage unbalance duration in all investigated cases and grids. Moreover, while it had some notable mitigation results in half of the investigated cases (PV-HP scenarios), its effectivity was proven uncertain in all scenarios that included EVs. While the further investigation of phase unbalance mitigation is out of the scope of this work, more sophisticated power-control measures (such as smart-charging and DSM), which can also alter the LCT phase connections in real-time, should be investigated to reach a final conclusion about the potential of voltage unbalance mitigation without the need of additional assets (e.g. ESSs) or grid reinforcements (e.g. higher cable area, etc.). In this regard, emerging phase-changing EV chargers, such as the Zaptec EV charger, can assist in the implementation of the power control strategies proposed above in practice.

VI. DISCUSSION OF RESULTS

A. SUMMARY OF FINDINGS

Compared with the knowledge in the existing literature, the findings of this work have been distinguished into the three following categories:

A) Findings in agreement.
B) Contradictory findings.
C) New findings.

1) A) IN AGREEMENT:

The significance of the unbalance impact due to LCT integration has also been shown in this work. Especially the unbalance impact increase due to combined LCT integration has been shown in multiple studies such as in [25] and [26] for PVs and EVs, in [29] and [30] for EVs and HPs, in [32] and [33] for PVs, EVs, and HPs, etc.

For example, the authors in [25] showed that the VUF exceeded 2% even from 20% combined penetrations of PVs and EVs for 28% and 31% of the simulation time during Winter and Summer, respectively, reaching a maximum value of 10% under 80% combined penetrations. Moreover, a higher VUF was found during Summer compared to Winter for all studied penetration levels showing higher violation that could reach up to 40%. This comes in agreement with our observation about higher voltage unbalance during Summer in our PV-EV scenarios. However, the authors in [25] did not include HPs in their investigation to show the HP contribution combined with the seasonal influences to voltage unbalance. Furthermore, voltage unbalance violations were investigated in [26] in rural and suburban grids during increasing combined EV and PV penetrations. While no violations were found for both grids, the suburban grids showed lower unbalance reserves for further EV and PV integration, when cables were considered for distribution lines in both grids. However, the investigated networks, while developed in coordination with the German DSOs, did not constitute real grids. Additionally, the authors in [30] found more pessimistic results, showing VUF violations even from 20% combined penetrations of EVs and HPs, which reached a maximum value of 12%. However, no PV integration and season comparison were performed in the study, neglecting the interrelations of the EVs and HPs with the PV generation simultaneously considering the impact of the seasonal effect.

In this work, the combined integration of PVs, EVs, and HPs provoked the highest voltage unbalance compared to the other LCT combinations, as was also seen in [32]. Compared to the maximum predicted unbalance of 4.1% under 100% combined penetration in [32], our unbalance results for the Dutch suburban grids are even more pessimistic, reaching a value up to 8%. This is justified by the overpopulation that characterizes the Dutch suburban grids; in contrast, an adapted network was investigated in [32]. Furthermore, while seasonal comparisons were ignored in [32], the authors investigated the effect of the cable size, showing that a 30% cable size decrease can result in 10% higher VUF; however, only the 100% penetration level was investigated in the study. Furthermore, a higher amount of violations was also identified in [33] during the combined integration of all PVs, EVs. and HPs. However, the authors showed how balanced power flows underestimate violations concerning voltage deviations, loading utilization, and energy losses, without directly measuring the unbalance in the investigated grids. For example, it was shown that voltage violations begin only at 90% PV-EV-HP penetration levels during balanced power flows, while the respective penetration level was only 40% during the case of unbalanced power flows. Moreover, the effects of different seasons and distribution grid types on phase unbalance were not quantified.

Moreover, the strong effect of the existing grid loading was also proven in this work by comparing light- and heavy-loaded grids of the same type. This comes in agreement with the findings in [30], where two Scottish urban grids (one large- and one small-sized) were compared, predicting a 100% higher maximum unbalance for the first one. Furthermore, the general influence of the increasing penetration levels on the voltage unbalance increase was also evident in this work since, in most cases, 100% LCT penetration had the most detrimental effect on unbalance, with 50% penetration level being the most important intermediate step for all studied LCT combinations. Such findings agree with the insights about the importance of the penetration level in the studies of [23], [24], [25], [26], [27], [29], [30], [31], and [33] for combined integration of PVs-EVs, EV-HPs, PVs-HPs & PVs-EVs-HPs, respectively.

Finally, the importance of the grid topology on voltage unbalance was also proven in this work. It was seen that DGs that comprise a high number of radial feeders are more prone to voltage unbalance due to higher voltage deviations by loads located at the feeders' ends (away from the transformer). This comes in agreement with similar observations made in [24], where the furthest point from the distribution transformer suffered from the highest unbalance. Furthermore, similar observations were made in [34], where the authors compared the contributions to voltage violations of PVs, EVs, and HPs, analyzing them both temporarily and spatially during unbalanced power flows. It was found that the customers located after the 40% feeder length caused the highest amount of violations.

2) B) CONTRADICTORY FINDINGS:

Firstly, regarding grid comparison, suburban grids were found to be more vulnerable to voltage unbalance, and they were the only DGs exceeding the legal limit of 3% VUF. On the contrary, LCT integration was less hazardous for rural and urban grids. This contradicts the findings in [27] where the the authors calculated the phase residual current in urban, suburban, and rural grids of the UK, finding an average value of 100A, 60A, and 40A, respectively. Hence, while the UK suburban grids were found more prone to unbalance than the UK rural grids, the urban grids were found to be the most vulnerable. Moreover, the authors in [26] found the German rural grid more vulnerable to unbalance than the investigated suburban grid (even from 50% of combined PV-EV penetrations); however, only when they considered overhead distribution lines for the rural grid. In contrast, as explained before, better results were seen for the rural grid when cables were considered for the distribution lines of both grids. In our case studies, the higher vulnerability of the suburban grids is justified by their overpopulation in the Netherlands which is multiple times higher than the Dutch rural and urban grids (see TABLE 2). Moreover, the studied heavy-loaded rural grid in our work showed an x2 times higher VUF than the respective heavy-loaded urban grid, which comes in agreement with the comparison between rural and urban grids in [27] and [31]. The above comparisons between the findings of our work and the existing knowledge show the high influence of the characteristics of the distribution grids of different countries, and hence, the results should not be generalized regarding grid-type comparisons. Therefore, a study investigating voltage unbalance in the same grid types of different countries could provide more conclusive insights concerning this matter.

Secondly, regarding LCT comparison, the HP integration provoked always higher voltage unbalance than the EV integration during Winter under all penetration levels. This finding contradicts with results in [30], where EV charging was found to be more hazardous for phase unbalance than HPs. More specifically, the VUF reached a value of 7% and 3% under 100% penetration level of EVs and HPs, respectively. However, the authors did not consider the seasonal effect and PV integration in their study, neglecting the seasonal LCT interrelations. Moreover, similar insights were also drawn in the two investigated LV feeders in [32], finding a maximum VUF of 2.9% and 3.4% during 100% EV integration and 2% and 2.5% during 100% HP integration for the two feeders, respectively. However, while PVs were included in this study, their co-integration was not considered in the above comparisons. Moreover, only one developed network was investigated in [32], and concerning the seasonal influence, the authors used Summer PV profiles and Winter EV profiles to investigate the worst-case scenario. In contrast, in our study, the higher impact of HP integration on voltage unbalance was justified by the fact that HP operation lasts longer than the fewer EV charging events since, in our modeling, we considered that the HPs continuously maintain the thermal comfort of the occupied buildings. Thus, this is also a direct effect of utilizing detailed models of the LCTs for the generation of their profiles (bottom-up studies) instead of using nationalized data (top-down studies) or more simplified formulas. Moreover, residential HPs are all single-phase connected in contrast with EV charging, which is performed single-phased only for rated power < 7.4kW. Finally, distinguishing Summer and Winter profiles for all LCTs, it was found that different seasons affect the inflicted unbalanced results differently by different LCT combinations; hence, while Winter is more hazardous for PV-HP integration, the opposite applies for Summer and PV-EV integration.

Thirdly, regarding season comparison, a slightly lower overall unbalance was seen during Summer compared to Winter for the combined PV-HP-EV integration cases. From the works in TABLE 1, only the work in [25] compared explicitly the unbalance results between Summer and Winter, and found the Summer season as the most hazardous for voltage unbalance by LCT integration. However, the authors in [25] did not include HPs in their investigation, which were found in our work to have a crucial effect on the total provoked unbalance between different seasons. If the results in [25] are compared with our results from the PVs-EVs scenarios, hence investigating the same LCTs, the findings of the two studies come in agreement.

Finally, taking everything into account, it can be concluded that these findings are highly case-specific and dependent on the characteristics of the study and should not be generalized over works with highly different case conditions. Nevertheless, they are valuable for distribution system operators (DSOs) in the Netherlands and should be taken into consideration for other countries with similar grid characteristics and weather conditions.

3) C) NEW FINDINGS:

The key new insights of this work are summarized as follows:

1) While the VUF generally increases during increasing LCT penetration levels, unbalance mitigation effects were observed for all LCT combinations in some penetration levels after 50% penetration. While this was seen in some works for the PVs-EVs combination ([22], [24]), it wasn't seen again for the PVs-HPs combination (e.g. in [31]) or the PVs-HPs-EVs combination ([32], [33], [34]). In our work, these mitigation effects without the use of any measures were seen because integrated LCTs at higher penetration levels can even out LCTs at lower levels if the extra load is added to a different phase.

2) The main effect of the LCT distribution unbalance factor concerns the unbalance variance, which was higher in the light-loaded grids than in their heavy-loaded grid counterparts. That means that the unbalance can deviate higher from the average value when LCT locations are altered in lighter-loaded grids; however, the insights from DG and LCT comparisons remained the same.

3) In balanced power flows, coincident operation of generators and loads (e.g. PVs and EVs) would most probably be beneficial for mitigation of violations. On the contrary, coincident LCT operation can become detrimental to unbalanced power flows if LCTs inject and withdraw power from different phases simultaneously. This is the reason why the unbalance provoked by PV-EV integration was considerably increased during Summer when PV generation is higher, while this was not observed for PV-HP integration; PVs and EVs overlap much higher than PVs and HPs.

4) Concerning unbalance factors' comparison, the seasonal effect was found to have a much higher influence on unbalance than the LCT grid distribution. While PV-HP integration caused a higher VUF than PV-EV integration during Winter at all penetration levels and DGs, PV-EV integration approximated and, in some levels, overpassed PV-HP integration during Summer (due to insight 3). On the contrary, LCT grid distribution, while increasing the unbalance variance, did not alter this work's main insights.

5) Consumption-based (thermal comfort decrease) and power-based (average charging) mitigation measures decreased the total duration of unbalance violations in a range between 11% and 25%.

6) Regarding consumption-level effect, the utilization of the thermal comfort decrease as a mitigation measure, decreased notably the VUF (up to 15% decrease). Mitigation of unbalance was seen in some works by power-based measures. For example, the authors in [24] reduced the unbalance from 5% to 3.5% using EV smart charging. This work is the first study in which a consumption-based measure (heating consumption decreased by a decrease in thermal comfort) provided notable unbalance mitigation. However, it did not manage to reduce the VUF below 3% for the heavy-loaded suburban grid.

7) Average charging caused contradictory results (increase and decrease) concerning the magnitude of unbalance violations. This was justified by the fact that average charging reduces the charging power levels while simultaneously increasing the charging duration (it expands the duration during the whole parking period). Hence, according to insight 3, the simultaneity of EV charging with other LCT operations (e.g. PV generation) can be increased and provoke higher voltage unbalance. Hence, more sophisticated power control strategies (such as phase-changing smart charging) should be investigated for unbalance mitigation.

8) From insights 3 & 7, we can conclude that while the duration of consumption is as important as peak power levels for phase unbalance, and hence, decreasing the peak power levels at the expense of duration (e.g. average charging) is not always effective.

B. CRITICAL VOLTAGE UNBALANCE RESULTS AND MITIGATION RECOMMENDATIONS

From the above analysis, it is concluded that uncontrolled phase integration of LCTs such as PVs, EVs, and HPs in future distribution grids can cause major unbalance issues, and several critical situations have been identified.

1. Due to high existing loading and overpopulation, suburban grids are highly vulnerable, especially at high combined penetrations of PVs, HPs, and EVs. It is important that, especially in heavy-loaded grids, such as in suburban areas, the LCT phase connection planning is coordinated beforehand during the LCT grid installations.

2. A high number of loads at the end of radial feeders can highly jeopardize voltage unbalance even in grids with lower loading, due to higher undervoltage compared with the nodes closer to the distribution transformer. Hence, overloading at the end of radial feeders should be avoided if possible, otherwise, the installation of additional assets, such as ESSs, could benefit high voltage deviations and, consequently, voltage unbalance.

3. Simultaneous LCT operation can be critical for unbalance, when LCTs operate in different phases. This was seen for EV integration during Summer due to higher overlap with PV generation (PV generation lasts longer during Summer) and it was also endorsed with the average EV charging results (average charging increases the duration of the EV charging). Hence, power-injecting and power-withdrawing LCTs whose operations overlap, such as PVs and EVs, respectively, should be considered to be connected at the same phase to reduce the impact on voltage unbalance. Furthermore, emerging phase-changing chargers can assist in solving unbalance by managing the LCT phase connections in real time.

4. HP integration can critically affect voltage unbalance, especially concerning heating during Winter seasons, when HP consumption levels are higher and are operated for a longer period during the day. Moreover, most residential HPs are single-phase devices. A first step in varying LCT power and consumption levels has been taken in this study which resulted in mitigating effects; however, to a limited extent. More sophisticated power/consumption control and DSM solutions capable of utilizing different price mechanisms should be investigated further for potential unbalance mitigation without the use of additional installations and/or grid reinforcements. Additionally, the further adoption of LCT 3-phase connections can further reduce phase unbalance.

Finally, grid investments and reinforcements (e.g. higher transformer capacities, larger cable cross-section areas, etc) are also recommended for unbalance mitigation if the less costly strategies are not adequate to keep voltage unbalance below the legal limit of 3%.

Overall, it was seen that different grid types, seasons, and weather conditions favor or deteriorate the inflicted unbalance of different integrated combinations of LCTs. In addition, the power injections and withdrawals by simultaneous LCT operation can magnify the unbalance issue further and are strongly dependent on the social adoption of LCTs and user behavior. Therefore, the developed mitigation solutions can highly differ and must be adapted to the needs of each distribution grid and its characteristics accounting simultaneously for a yearly analysis.

C. LIMITATIONS

Taking everything into consideration, this work's limitations can be summarized as follows:

The work has incorporated a level of uncertainty in the grid unbalance assessment. For example, as discussed, MCS was utilized for the generation of 600 home, semi-public, and public EV charging profiles, while random PV orientations and building occupancy profiles were used for the generation of the 90 PV and 200 HP profiles. Moreover, the weather data acquired by the Meteonorm database, such as solar irradiation and ambient temperature, are averaged over the duration of the last 10 years. However, there are a lot of other sources of uncertainty that were not considered in the analysis. Some examples are the consideration of different PV and HP modules, different types of buildings and building parameters, a higher number of distribution grids per category, etc.

Furthermore, on the one hand, the utilization of the Dutch distribution grids contributes to the unbalance analysis of different grid types and LCT distributions considering real-world data and not synthesized test feeders. On the other hand, it decreases the level of generalization in some of the previously explained findings. The same also applies with the use of the Dutch weather conditions. Therefore, the contradictory findings in Section VI-A.2. regarding DG and LCT comparisons apply mostly to the country of the Netherlands and at a level for countries with similar grid characteristics and weather conditions. However, the findings in Sections VI-A.1. and VI-A.3., such as the importance of the grid topology, comparisons between different unbalance factors and the importance of the seasonal effect, the mitigation potential of LCT power and consumption levels, etc, can be generalized for grid unbalance assessment studies and are independent of the grid and weather conditions of this work.

Additionally, as already discussed, the alteration of the LCT power and consumption levels have been investigated as mitigation solutions for the grid unbalance. However, only one power-level solution (average charging) and one consumption-level solution (decrease of buildings' thermal comfort) have been included in the study. Further solutions in this regard should be studied in order to conclude about the effectivity of LCT power and consumption levels on their inflicted unbalance.

Finally, this work did not consider social acceptance factors in the analysis. For example, the LCT distribution was realized homogeneously, while in reality, people living in higher-income areas tend to adopt new technologies more easily, leading to a skewed distribution. Moreover, a household with a PV system is more likely to also own an EV and/or an HP; however, in this work, a building may own a PV rooftop and not an EV or an HP and vice versa.

VII. CONCLUSION AND FUTURE WORK

This work has followed a bottom-up approach to evaluate the inflicted phase unbalance by the integration of PVs, EVs, and HPs on different types of Dutch LV DGs (rural, urban, and suburban) under different combinations and penetration levels. Focus has been placed on the quantification of the influence of 4 main unbalance factors on the interrelated inflicted unbalance by the different LCT combinations: the LCT phase connections and grid distributions, the seasonal effect, and the LCT power and consumption levels. The use of the latter as a mitigation measure has also been evaluated.

The Dutch suburban grids were found to be the most vulnerable in future phase unbalance. Moreover, the seasonal effect significantly enhanced the provoked unbalance by PV-HP and PV-EV integration during Winter and Summer, respectively. While LCT grid distribution showed a notable effect on the unbalance variance, it was less impactful on the overall unbalance observations concerning grid and LCT comparisons. Regarding the mitigation strategies, the decrease in the LCT consumption level decreased the magnitude of the unbalance violation and, remarkably, its duration. Finally, it was found that the increase of consumption duration can be as detrimental to unbalance as the power levels, because it can increase the simultaneity factor of LCTs that operate in different phases.

In future work, a higher level of uncertainty in the analysis is recommended to study its impact on the unbalance results (e.g. different LCT and building properties, etc.). Furthermore, the use of more real-world rural, suburban, and urban DGs, preferably from a different country than the Netherlands, is proposed to ensure the generalization of results. Finally, it was seen that the effect of LCT power and consumption levels as mitigation can be contradictory. While further investigation of phase unbalance mitigation is out of the scope of this work, further power and consumption control strategies with the use of phase-changing devices (such as EV chargers) are recommended for future work to conclude about the effectiveness of mitigation measures without additional assets of reinforcements for phase unbalance.

ACKNOWLEDGMENT

Moreover, the authors would like to thank Enexis Groep for the provision of the six distribution grids.

REFERENCES

[1] C. Fetting, "The European green deal," Eur. Sustain. Develop. Netw. Office (ESDN), Vienna, Austria, Tech. Rep. 2, 2020.

[2] P. Bojek, "Solar PV global supply chains," Int. Energy Agency, Paris, France, Tech. Rep., 2022.

[3] L. Cozzi, "The future of heat pumps," Int. Energy Agency, Paris, France, Tech. Rep., 2022.

[4] O. Alsauskas, E. Connelly, A. Daou, A. Gouy, M. Huismans, H. Kim, J. Le Marois, S. McDonagh, A. Petropoulos, and J. Teter, "Global EV outlook 2023," Int. Energy Agency, Paris, France, Tech. Rep., 2023.

[5] *Regulation (EU) 2023/851 of the European Parliament and of the Council*, E. U. Council E. U. Parliament, Brussel, Belgium, May 2023, p. 5.

[6] *Capacity Map in the Electricity Grid*. Accessed: 10, 24, 2023. [Online]. Available: https://capaciteitskaart.netbeheernederland.nl/

[7] (2023). *Electricity Code: Article 2.33*. [Online]. Available: https://wetten.overheid.nl/jci1.3: c: BWBR0037940&hoofdstuk=2&paragraaf=2.4&artikel=2.33&z=2023-05-11&g=2023-05-11

[8] J. Conzade, F. Nägele, S. Ramanathan, and P. Schaufuss, "Europe's EV opportunity–and the charging infrastructure needed to meet it," McKinsey, New York, NY, USA, Tech. Rep., 2022.

[9] (2022). *NEN-En 50160 Voltage Characteristics of Electricity Supplied By Public Electricity Networks*. [Online]. Available: https://standards.globalspec.com/std/14579674/NEN-EN%2050160

[10] K. Ma, L. Fang, and W. Kong, "Review of distribution network phase unbalance: Scale, causes, consequences, solutions, and future research directions," *CSEE J. Power Energy Syst.*, vol. 6, no. 3, pp. 479–488, Sep. 2020.

[11] E. Clarke, "Simultaneous faults on three-phase systems," *Trans. Amer. Inst. Electr. Engineers*, vol. 50, no. 3, pp. 919–939, Sep. 1931.

[12] K. Ma, R. Li, and F. Li, "Quantification of additional asset reinforcement cost from 3-Phase imbalance," *IEEE Trans. Power Syst.*, vol. 31, no. 4, pp. 2885–2891, Jul. 2016.

[13] F. J. Ruiz-Rodriguez, J. C. Hernández, and F. Jurado, "Voltage unbalance assessment in secondary radial distribution networks with single-phase photovoltaic systems," *Int. J. Electr. Power Energy Syst.*, vol. 64, pp. 646–654, Jan. 2015. [Online]. Available: https://www.sciencedirect.com/science/article/pii/S0142061514005158

[14] O. Mrehel and A. A. Issa, "Voltage imbalance investigation in residential LV distribution networks with rooftop PV system," in *Proc. IEEE 2nd Int. Maghreb Meeting Conf. Sci. Techn. Autom. Control Comput. Eng. (MI-STA)*, May 2022, pp. 655–662.

[15] G. Chicco, F. Corona, R. Porumb, and F. Spertino, "Experimental indicators of current unbalance in building-integrated photovoltaic systems," *IEEE J. Photovolt.*, vol. 4, no. 3, pp. 924–934, May 2014.

[16] K. Girigoudar and L. A. Roald, "On the impact of different voltage unbalance metrics in distribution system optimization," *Electr. Power Syst. Res.*, vol. 189, Dec. 2020, Art. no. 106656. [Online]. Available: https://www.sciencedirect.com/science/article/pii/S0378779620304594

[17] A. Ul Haq, C. Cecati, K. Strunz, and E. Abbasi, "Impact of electric vehicle charging on voltage unbalance in an urban distribution network," *J. Intell. Robotic Syst.*, vol. 1, pp. 51–60, May 2015.

[18] L. Mejdi, F. Kardous, and K. Grayaa, "Impact analysis and optimization of EV charging loads on the LV grid: A case study of workplace parking in Tunisia," *Energies*, vol. 15, no. 19, p. 7127, Sep. 2022.

[19] S. Z. Moghaddam and T. Akbari, "A mixed-integer linear programming model for the plug-in electric vehicle charging problem in unbalanced low voltage electrical distribution systems considering neutral conductor," *Electr. Power Syst. Res.*, vol. 209, Aug. 2022, Art. no. 108049. [Online]. Available: https://www.sciencedirect.com/science/article/pii/S0378779622002747

[20] A. S. Türkoğlu, H. C. Güldorum, I. Sengor, A. Çiçek, O. Erdinç, and B. P. Hayes, "Maximizing EV profit and grid stability through virtual power plant considering V2G," *Energy Rep.*, vol. 11, pp. 3509–3520, Jun. 2024. [Online]. Available: https://www.sciencedirect.com/science/article/pii/S2352484724001586

[21] A. Navarro-Espinosa and P. Mancarella, "Probabilistic modeling and assessment of the impact of electric heat pumps on low voltage distribution networks," *Appl. Energy*, vol. 127, pp. 249–266, Aug. 2014. [Online]. Available: https://www.sciencedirect.com/science/article/pii/S030626191400378X

[22] M. A. Essa, "Power quality of electrical distribution systems considering PVs, EVs and DSM," *J. Control, Autom. Electr. Syst.*, vol. 31, no. 6, pp. 1520–1532, Dec. 2020.

[23] A. A. Raouf Mohamed, R. J. Best, D. John Morrow, A. Cupples, and I. Bailie, "Impact of the deployment of solar photovoltaic and electrical vehicle on the low voltage unbalanced networks and the role of battery energy storage systems," *J. Energy Storage*, vol. 42, Oct. 2021, Art. no. 102975. [Online]. Available: https://www.sciencedirect.com/science/article/pii/S2352152X21006897

[24] P. Rodríguez-Pajarón, A. Hernández, and J. V. Milanović, "Probabilistic assessment of the impact of electric vehicles and nonlinear loads on power quality in residential networks," *Int. J. Electr. Power Energy Syst.*, vol. 129, Jul. 2021, Art. no. 106807.
[25] T. Antić, T. Capuder, and M. Bolfek, "A comprehensive analysis of the voltage unbalance factor in PV and EV rich non-synthetic low voltage distribution networks," *Energies*, vol. 14, no. 1, p. 117, Dec. 2020.
[26] S. Mueller, F. Moeller, M. Klatt, J. Meyer, and P. Schegner, "Impact of large-scale integration of E-mobility and photovoltaics on power quality in low voltage networks," in *Proc. Int. ETG Congr.*, Nov. 2017, pp. 1–6.
[27] W. Kong, K. Ma, and F. Li, "Probabilistic impact assessment of phase power imbalance in the LV networks with increasing penetrations of low carbon technologies," *Electr. Power Syst. Res.*, vol. 202, Jan. 2022, Art. no. 107607. [Online]. Available: https://www.sciencedirect.com/science/article/pii/S0378779621005885
[28] F. M. Uriarte and Robert. E. Hebner, "Residential smart grids: Before and after the appearance of PVs and EVs," in *Proc. IEEE Int. Conf. Smart Grid Commun. (SmartGridComm)*, Nov. 2014, pp. 578–583.
[29] Y. Li and P. A. Crossley, "Monte Carlo study on impact of electric vehicles and heat pumps on LV feeder voltages," in *Proc. 12th IET Int. Conf. Develop. Power Syst. Protection (DPSP)*, Mar. 2014, pp. 1–6.
[30] C. McGarry, A. Anderson, I. Elders, and S. Galloway, "A scalable geospatial data-driven localization approach for modeling of low voltage distribution networks and low carbon technology impact assessment," *IEEE Access*, vol. 11, pp. 64567–64585, 2023.
[31] S. Meunier, C. Protopapadaki, R. Baetens, and D. Saelens, "Impact of residential low-carbon technologies on low-voltage grid reinforcements," *Appl. Energy*, vol. 297, Sep. 2021, Art. no. 117057. [Online]. Available: https://www.sciencedirect.com/science/article/pii/S0306261921005146
[32] M. J. M. Al Essa and L. M. Cipcigan, "Integration of renewable resources into low voltage grids stochastically," in *Proc. IEEE Int. Energy Conf. (ENERGYCON)*, Apr. 2016, pp. 1–5.
[33] A. Navarro and L. Ochoa, "Deliverable 3.6 'What-if scenario impact studies based on real LV networks,'" Electr. North West Ltd. (ENWL), Stockport, U.K., Tech. Rep., 2014.
[34] B. Fritz, G. Sampaio, and R. J. Bessa, "Data-driven assessment of the DER flexibility impact on the LV grid management," in *Proc. IEEE Belgrade PowerTech*, Jun. 2023, pp. 1–6.
[35] D. Fischer, A. Surmann, and K. B. Lindberg, "Impact of emerging technologies on the electricity load profile of residential areas," *Energy Buildings*, vol. 208, Feb. 2020, Art. no. 109614. [Online]. Available: https://www.sciencedirect.com/science/article/pii/S0378778819309594
[36] P. Pillay and M. Manyahe, "Definitions of voltage unbalance," *IEEE Power Eng. Rev.*, vol. 21, no. 5, pp. 49–51, May 2001.
[37] (2023). *Electricity Code: Article 7.3c*. [Online]. Available: https://wetten.overheid.nl/jci1.3: c: BWBR0037940&hoofdstuk=7&paragraaf=7.2&artikel=7.3&z=2023-05-11&g=2023-05-11
[38] NEDU. (2018). *Profielen Elektriciteit 2018*. [Online]. Available: https://web.archive.org/web/20181202215314/https://www.nedu.nl/documenten/verbruiksprofielen/
[39] N. Damianakis, G. R. C. Mouli, P. Bauer, and Y. Yu, "Assessing the grid impact of electric vehicles, heat pumps & PV generation in Dutch LV distribution grids," *Appl. Energy*, vol. 352, Dec. 2023, Art. no. 121878. [Online]. Available: https://www.sciencedirect.com/science/article/pii/S0306261923012424
[40] A. H. Smets, K. Jäger, O. Isabella, R. Van Swaaij, and M. Zeman, *Solar Energy: The Physics and Engineering of Photovoltaic Conversion Technologies and Systems*. Cambridge, U.K.: UIT, 2016.
[41] *Meteonorm*. Accessed: May 9, 2022. [Online]. Available: https://meteonorm.com/en/
[42] *Elaadnl Open Datasets for Electric Mobility Research*. Accessed: May 26, 2022. [Online]. Available: https://platform.elaad.io/analyses/ElaadNLopendata.php
[43] Y. Yu, D. Reihs, S. Wagh, A. Shekhar, D. Stahleder, G. R. C. Mouli, F. Lehfuss, and P. Bauer, "Data-driven study of low voltage distribution grid behaviour with increasing electric vehicle penetration," *IEEE Access*, vol. 10, pp. 6053–6070, 2022.
[44] N. Damianakis, Y. Yu, G. C. R. Mouli, and P. Bauer, "Frequency regulation reserves provision in EV smart-charging," in *Proc. IEEE Transp. Electrific. Conf. Expo (ITEC)*, Jun. 2023, pp. 1–6.
[45] N. Damianakis, G. C. R. Mouli, and P. Bauer, "Risk-averse estimation of electric heat pump power consumption," in *Proc. IEEE 17th Int. Conf. Compat., Power Electron. Power Eng. (CPE-POWERENG)*, Jun. 2023, pp. 1–6.
[46] *Enexis, 'S-Hertogenbosch*. Accessed: Feb. 25, 2022. [Online]. Available: https://www.enexis.nl/
[47] B. Thormann and T. Kienberger, "Evaluation of grid capacities for integrating future E-mobility and heat pumps into low-voltage grids," *Energies*, vol. 13, no. 19, p. 5083, Sep. 2020.
[48] G. R. Chandra Mouli, M. Kefayati, R. Baldick, and P. Bauer, "Integrated PV charging of EV fleet based on energy prices, V2G, and offer of reserves," *IEEE Trans. Smart Grid*, vol. 10, no. 2, pp. 1313–1325, Mar. 2019.

YME WESSELING (Member, IEEE) received the B.Sc. degree in electrical engineering and the M.Sc. degree in sustainable energy technology from the Technical University of Delft, in 2020 and 2023, respectively. He is currently an Engineer with Movares Nederland B.V., Utrecht, The Netherlands.

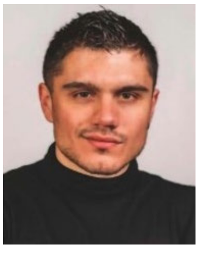

NIKOLAOS DAMIANAKIS (Member, IEEE) received the joint B.Sc. and M.Sc. degrees in electrical engineering from the National Technical University of Athens, in 2018, and the M.Sc. degree in electrical power engineering from the Technical University of Delft, in 2021. He is currently pursuing the Ph.D. degree in coordinated power control of smart loads and energy storage systems in dc power grids with the DC Systems, Energy Conversion, and Storage Group, Electrical Sustainable Energy Department, Delft University of Technology.

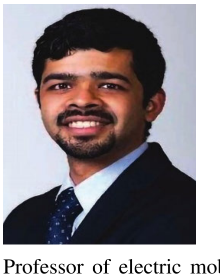

GAUTHAM RAM CHANDRA MOULI (Member, IEEE) received the bachelor's degree in electrical engineering from the National Institute of Technology, Trichy, India, in 2011, the master's degree in electrical engineering from Delft University of Technology, in 2013, and the Ph.D. degree from Delft University, in 2018, for the development of a solar-powered V2G electric vehicle charger with smart charging, compatible with CHAdeMO and CCS/COMBO. He is currently an Assistant Professor of electric mobility with the DC Systems, Energy Conversion, and Storage Group, Department of Electrical Sustainable Energy, Delft University of Technology. His current research interests include electric vehicles, EV charging, batteries, power electronics, and grid integration.

PAVOL BAUER (Senior Member, IEEE) received the master's degree in electrical engineering from the Technical University of Kosice, in 1985, and the Ph.D. degree from Delft University of Technology, in 1995. He is currently a Full Professor with the Department of Electrical Sustainable Energy, Delft University of Technology, and the Head of the DC Systems, Energy Conversion, and Storage Group. From 2002 to 2003, he worked partially at KEMA (DNV GL, Arnhem) on different projects related to power electronics applications in power systems. He is a member of the Executive Committee of the European Power Electronics Association (EPE). He is a former Chair of the Benelux IEEE Joint Industry Applications Society, the Power Electronics and Power Engineering Society Chapter, and the Power Electronics and Motion Control (PEMC) Council.